PERGAMON

Journal of the Mechanics and Physics of Solids
49 (2001) 2839–2875

JOURNAL OF THE
MECHANICS AND
PHYSICS OF SOLIDS

www.elsevier.com/locate/jmps

Feeding and dissipative waves in fracture and phase transition. III. Triangular-cell lattice

L.I. Slepyan *

Department of Solid Mechanics, Materials and Systems, Faculty of Engineering, Tel Aviv University, P.O. Box 39040, Ramat Aviv 69978 Tel Aviv, Israel

Received 2 February 2001; received in revised form 3 April 2001; accepted 3 April 2001

Abstract

Wave configurations for modes I and II of crack propagation in an elastic triangular-cell lattice are studied. [Mode III was considered in Part I of the paper: Slepyan, L.I. Feeding and dissipative waves in fracture and phase transition. I. Some 1D structures and a square-cell lattice. J. Mech. Phys. Solids 49 (2001) 469.] A general solution incorporates a complete set of the feeding and dissipative waves. The solution is based on the wave dispersion dependences obtained in an explicit form. Also some general properties and the long-wave asymptotes of the corresponding Green function are found. This results in the determination of the wavenumbers and modes. The macrolevel-associated solutions exist as the sub-Rayleigh crack speed regime for both modes and as a shear-longitudinal wave-speed intersonic regime for mode II only. In particular, it is shown that any intersonic crack speed is possible, whereas only the speed (shear wave speed multiplied by $\sqrt{2}$) corresponds to a positive energy release in the cohesive-zone-free homogeneous-material model. This is a manifestation of the fact that the local energy release in the lattice is not connected with the singularity of the macrolevel field. Microlevel solutions, corresponding to a nonzero feeding wavenumber, exist for both modes, at least from the energy point of view, for any, sub- and super-Rayleigh, intersonic and supersonic crack speed regimes. In particular, in the super-Rayleigh regime, a high-frequency wave delivers energy to the crack, while the macrolevel wave carries energy away from the crack.

Keywords: A. Dynamics; B. Crack mechanics; Lattice; C. Integral transforms

1. Introduction

In part I of this series (Slepyan, 2001a), the crack propagation in an elastic square-cell lattice was considered as a process caused by *feeding* waves, carrying energy to the

* Tel.: +972-3640-6224; fax: +972-3640-7617.
E-mail address: leonid@eng.tau.ac.il (L.I. Slepyan).

0022-5096/01/$ - see front matter
PII: S0022-5096(01)00053-9

crack front, and accompanied by *dissipative* waves carrying a part of this energy away from the front (the difference is spent on the bond disintegration). A complete set of steady-state, macrolevel-associated solutions (solutions of a zero feeding wavenumber) and genuine microlevel solutions (each of a nonzero wavenumber) for mode III crack propagation was represented. Part II (Slepyan, 2001b) was devoted to the study of similar wave configurations for phase transition dynamics.

In the present work, the last part of the series, modes I and II of crack propagation in a triangular-cell lattice are considered. The first analytical solution for crack propagation in the triangular-cell lattice was obtained in Kulakhmetova et al. (1984) where the total dissipation was found for the case of the sub-Rayleigh macrolevel-associated solution. Stability of crack propagation in this lattice was examined by Marder and Gross (1995). Some other related works were referenced in Part I of the paper (Slepyan, 2001a). Note that recently Gerde and Marder (2001) have successfully used this lattice model for the study of friction as mode II quasi-static fracture.

In the case of the triangular-cell lattice, the main relations are much more complicated than those for the square-cell lattice. However, fortunately wave dispersion dependences are found in an explicit form. This allows us to determine the feeding and dissipative wavenumbers and wave modes as in the case of the square-cell lattice.

The below-considered macrolevel-associated solutions exist only for the sub-Rayleigh crack speed (for both modes) and intersonic regions (for mode II). Both these regions are under consideration. While in the homogeneous-material model (without a cohesive zone), mode II intersonic crack can propagate only with the speed, $\sqrt{2}c_2$, any crack speed in the shear-longitudinal wave-speed region is possible in the lattice model. In a sense, this is as for the cohesive-zone homogeneous model. The lattice model possesses, however, more possibilities. In particular, it describes dissipative waves radiated by the propagating crack and microlevel feeding waves allowing the crack to propagate in the case where there is no macrolevel energy release. An inhomogeneous solution for the crack loaded by macrolevel distributed forces shows a finite local-to-global energy release ratio in a wide intersonic range.

Intersonic crack propagation in an elastic homogeneous material was considered in a number of works, in particular, in Burridge et al. (1979), Freund (1979), Slepyan (1981), Broberg (1999), Gao et al. (1999). Numerical simulations and experiments also show a possibility of the intersonic crack propagation (Rosakis et al., 1998; Needleman and Rosakis, 1999; Rosakis et al., 1999; Abraham and Gao, 2000).

The microlevel solutions are derived indiscriminately for sub- and super-Rayleigh ($0 < v < c_R$ and $c_R < V < c_2$), intersonic ($c_2 < v < c_1$) and supersonic ($v < c_1$) crack propagation. Here and below c_R, c_2 and c_1 are the Rayleigh wave, shear wave and longitudinal wave speeds, respectively (the same notations are used for the corresponding nondimensional values). Note that in the homogeneous-material model (with or without a cohesive zone) the super-Rayleigh crack speed is forbidden since the macrolevel wave corresponds to a negative energy release. In contrast, the lattice model, at least from the energy point of view, admits a super-Rayleigh solution. It corresponds to a microlevel feeding wave and includes the macrolevel wave as a dissipative one.

The lattice consists of particles connected by massless bonds (Fig. 1(a)). A semi-infinite crack is assumed to propagate to the right with a constant speed, v, that is, with

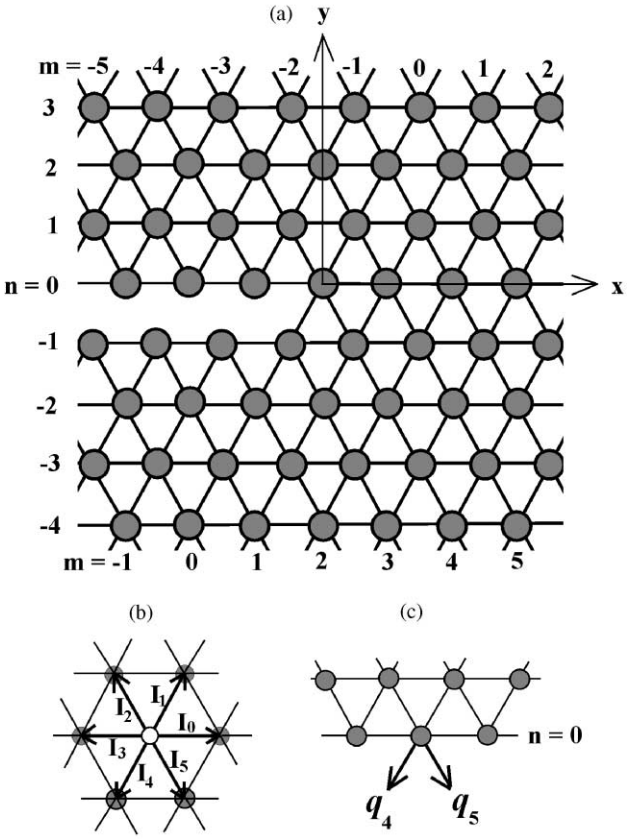

Fig. 1. The lattice: (a) the lattice and the coordinates; (b) the unit vectors and; (c) the external forces acting on the crack surface, $n=0$ (only one loaded particle is shown).

a constant time-interval between the disintegration of neighboring bonds on the crack path, $a/(2v)$. The solution corresponds to cutting of the bonds with a given speed.

In solving the problem, some general properties of the Green function are established without inspection of its specific structure. This allows us to use an analytical technique, the same as in part I, without detailed analysis of this complicated function.

2. General properties of fundamental solutions

2.1. The lattice and coordinates

In this lattice (Fig. 1(a)), each particle of mass M is connected with six neighbors by the same elastic bonds, each of the length a and stiffness μ. In the long-wave/low-frequency approximation, the lattice corresponds to a two-dimensional, homogeneous, isotropic, elastic body with density $\rho=2M/(\sqrt{3}a^2)$, Poisson's ratio $v=1/3$ and the

following velocities of the longitudinal, shear and Rayleigh waves: $c_1=\sqrt{9/8}c$, $c_2=\sqrt{3/8}c$ and $c_R=\frac{1}{2}\sqrt{3-\sqrt{3}}c$, respectively, where $c=a\sqrt{\mu/M}$. The shear modulus is $\mu_0=\rho c_2^2=\sqrt{3}\mu/4$.

In the following, we use nondimensional values associated with the natural units of the system: the particle mass ($M=1$), the bond length ($a=1$) and the bond stiffness ($\mu=1$). In these terms, c is the speed unit ($c=1$), a/c is the time unit, $\rho=2/\sqrt{3}$, $c_1=\sqrt{9/8}$, $c_2=\sqrt{3/8}$ and $c_R=\frac{1}{2}\sqrt{3-\sqrt{3}}$.

Coordinates of the particles are defined by the position vector

$$\boldsymbol{x}'=m\boldsymbol{I}_0+n\boldsymbol{I}_1, \tag{1}$$

where m and n are integer numbers, and $\boldsymbol{I}_p$, $p=0,1,\ldots,5$, are the unit vectors directed from a given particle to the neighboring ones (Fig. 1(b)). In terms of the projections onto the x, y-axis shown in Fig. 1(a) these vectors are

$$\boldsymbol{I}_p=[\cos(\pi p/3),\sin(\pi p/3)]. \tag{2}$$

According to this we may use both the rectangular coordinates, $x=m+n/2$, $y=\sqrt{3}n/2$, and the m,n-system.

The crack propagation is a consequence of disintegration of the bonds between lines $n=0$ and $n=-1$. These bonds correspond to the vectors $\boldsymbol{I}_4$ and $\boldsymbol{I}_5$—for the particles with $n=0$ or the vectors $\boldsymbol{I}_1$ and $\boldsymbol{I}_2$—for the particles with $n=-1$.

2.2. Integral transform in the moving coordinate system

For the considered steady-state problem, we assume that displacements of the particles depend on two variables only: y and $\eta=x-Vt$, where $V=v/c$ is the nondimensional crack speed. Along with this, the steady-state solution is considered as a limit, $t\to\infty$, $\eta=const$, of a transient solution which corresponds to zero initial conditions. Accordingly, the Fourier transform in the moving coordinate system

$$\boldsymbol{u}^F=\int_{-\infty}^{\infty}\boldsymbol{u}(\eta,y)e^{ik\eta}\,d\eta \tag{3}$$

is considered as a limit of the Laplace and Fourier double transform. To show the connection let us first introduce an x-continuous representation of the displacements, $\boldsymbol{u}_0(t,x,y)$. The discrete Fourier transform is

$$\boldsymbol{u}_0^D(t,k,y)=\sum_x\boldsymbol{u}_0(t,x,y)\exp(ikx), \tag{4}$$

where $x=m+n/2$, $m=0,\pm1,\ldots$. The inverse transform is

$$\boldsymbol{u}_0(t,x,y)=\frac{1}{2\pi}\int_{-\pi}^{\pi}\boldsymbol{u}_0^D(t,k,y)\exp(-ikx)\,dk. \tag{5}$$

The function $\boldsymbol{u}_0(t,x,y)$ in the last equation can be treated as a function of x as a continuous variable with the Laplace and Fourier double transform as

$$\boldsymbol{u}_0^{LF}(s,k,y)=\int_0^{\infty}\int_{-\infty}^{\infty}\boldsymbol{u}_0(t,x,y)\exp(-st+ikx)\,dx\,dt. \tag{6}$$

Substitutions

$$x = \eta + Vt, \quad \mathrm{d}x = \mathrm{d}\eta, \quad s = s' + \mathrm{i}kV \tag{7}$$

lead to the double transform in the moving coordinate system

$$\boldsymbol{u}_0^{\mathrm{LF}}(s' + \mathrm{i}kV, k) = \int_0^\infty \int_{-\infty}^\infty \boldsymbol{u}_0(t, \eta + Vt, y)\exp(-s't + \mathrm{i}k\eta)\,\mathrm{d}\eta\,\mathrm{d}t. \tag{8}$$

If the steady-state limit exists then

$$\boldsymbol{u}^{\mathrm{F}} = \lim_{s' \to 0} s'\boldsymbol{u}_0^{\mathrm{LF}}(s' + \mathrm{i}kV, k, y). \tag{9}$$

Note that the multiplier, s' in this relation is canceled by the multiplier $1/s'$ as the Laplace transform of the unit step function, $H(t)$, in the expression of the load as $q(\eta)H(t)$. Thus the expression $0 + \mathrm{i}kV$ used below means the corresponding limit with $0+$ as the trace of its origin, while any function of the form $f(s' + \mathrm{i}kV, k)$ is the double transform (multiplied by s') in the moving coordinate system, where s' is the parameter the Laplace transform with respect to time ($\eta = \mathrm{const}$) and k is the parameter of the Fourier transform with respect to η ($t = \mathrm{const}$). This definition of the steady-state solution follows from the causality principle (see Appendix A in part I of the paper, Slepyan, 2001a).

2.3. Plan of the solution

The goal is to find possible wave configurations and to describe both the macrolevel and microlevel solutions. Such a solution, being found for any given crack speed, allows one to determine the speed if a feeding wave or the global energy release rate as well as the fracture criterion are given. In outline, the plan of the solution is as follows.

At first, the intact lattice is considered. This allows a general solution of an exponential type to be derived. Further, the equations for the particles forming the boundary of the upper half-plane, $n = 0$, are considered. At the crack, these particles are connected with four neighbors only, while there are six connections for each particle outside the crack. In addition, in the dynamic equations for these particles, nonspecified external forces, q, directed along the bonds (or a trace of a broken bond), are introduced—for convenience in an initial stage of the considerations (see Fig. 1(c) where the forces are shown only for one of the loaded particles).

As a result, a relation between the Fourier transform of the forces and the elongation of a bond on the crack path, Q^{F}, is obtained. Note that elongation of any other bond on the crack path is the same but with a shift in time depending on its location (in fracture mode II, lengthening and shortening alternate). At the crack, it is the elongation of the distance between the corresponding particles. This relation can be expressed as

$$Q^{\mathrm{F}} \equiv Q_+ + Q_- = f(s' + \mathrm{i}kV, k)(Q_+ + q^{\mathrm{F}}), \tag{10}$$

where Q_+ is the right-side Fourier transform of the elongation (related to the crack continuation), while Q_- is the left-side transform (related to the crack).

The Laplace and Fourier double transform $f(s' + \mathrm{i}kV, k)$ or to be more precise, a half of it, can be called the fundamental solution (or Green function) for the lattice

half-plane. Indeed, because of symmetry, this relation with $q^{\mathrm{F}} = 1$ $[q = \delta(\eta)]$ and zero *force* Q_+ on the right hand side of Eq. (10) represents the corresponding projections of the displacements of the upper half-plane boundary. The dynamic equations for the lattice are used just for the determination of this function.

From relation (10) we come to the governing equation for the lattice with a propagating crack:

$$L(s' + \mathrm{i}kV, k)Q_+ + Q_- = [1 - L(s' + \mathrm{i}kV, k)]q^{\mathrm{F}}, \tag{11}$$

where the crack-related Green function is

$$L(s' + \mathrm{i}kV, k) = 1 - f(s' + \mathrm{i}kV, k). \tag{12}$$

The next step is the transition to a homogeneous problem. This is made using a procedure where $q(\eta) \to 0$ with a nonzero limit of the right hand side of Eq. (11). In this way, existence of zero points of $L(0 + \mathrm{i}kV, k)$ and $1/L(0 + \mathrm{i}kV, k)$ is important, and the corresponding dependences as dispersion relations for waves in the lattice plane and the lattice half-plane are derived. Fortunately it appears that these relations can be expressed in an explicit form.

Finally, using the Wiener–Hopf technique a general solution and macrolevel-associated and microlevel solutions for different crack-speed regions are determined.

2.4. Some properties of the fundamental solutions

In the following, in connection with the use of the Wiener–Hopf technique, Arg $L(s' + \mathrm{i}kV, k)$ for L as a complex function will be needed. However, this function is so complicated that a direct analysis of it is too difficult. At the same time, some properties of it which help much for the determination of Arg $L(s' + \mathrm{i}kV, k)$ can be learned using general considerations, without inspection of its specific expression.

With this in mind, because some of the properties are true not only for the considered lattice but in a general case, consider a linear dynamic problem for the upper half-plane filled by an elastic or viscoelastic material of a general structure (in particular, a homogeneous medium) which allows a steady-state solution to exist. We assume that the material is *passive*, that is it can transfer and, possibly, absorb energy but cannot produce it.

Let $q_f(t,x)$ be a distributed external force acting on the half-plane boundary and $u(t,x)$ be the corresponding displacement directed opposite (as σ_{yy} (σ_{yx}) and u_y (u_x) in the case of a homogeneous material). We assume that under zero initial conditions the Laplace and Fourier double transform at $y = 0$ leads to the relation

$$u^{\mathrm{LF}}(s,k) = U^{\mathrm{LF}}(s,k)q_f^{\mathrm{LF}}(s,k). \tag{13}$$

Let us take the force as

$$q = q_f = q_0(\eta)\exp(s_0 t)H(t), \quad s_0 > 0. \tag{14}$$

The double transform in the moving coordinate system is then

$$u^{\mathrm{LF}}(s'+\mathrm{i}kV,k)=U^{\mathrm{LF}}(s'+\mathrm{i}kV,k)\,\frac{q_0^{\mathrm{F}}}{s'-s_0}. \tag{15}$$

Note that the fundamental solution, $U(t,x)$, corresponds to the displacement under the external force $\delta(x)\delta(t)$. Such action results in a displacement field *propagating* from the force. The Fourier transform of the field, due to passivity of the material, is a *slow-growing* function of t if $\Im k=0$ (it is assumed that k is real except as otherwise noted). The Laplace transform of such function is a regular function of s in the right half-plane, $\Re s>0(\Re s'>0)$. An asymptote of $u^{\mathrm{F}}(t,k)$ for $t\to\infty,\ \eta=\text{const.}$ is defined by the double transform (15) as a contribution of the singular point in s'-plane with the greatest real part, that is $s'=s_0$. Thus

$$u^{\mathrm{F}}=U^{\mathrm{LF}}(s_0+\mathrm{i}kV,k)q_0^{\mathrm{F}}\exp(s_0t). \tag{16}$$

Now consider a mixed problem where the displacements at $\eta>0$ cause forces (with a constant coefficient of proportionality denoted here by μ). In this case, denoting the total forces acting on the upper half-plane as q_t and the real external forces as q, we have

$$(q_t)_+=\mu u_++q_+,\quad (q_t)_-=q_-,\quad q_++q_-=q^{\mathrm{F}}. \tag{17}$$

We obtain the governing equation

$$L(s'+\mathrm{i}kv,k)u_++u_-=[1-L(s'+\mathrm{i}kv,k)]q^{\mathrm{F}}/\mu \tag{18}$$

with the crack-related Green function

$$L(s'+\mathrm{i}kv,k)=1-\mu U^{\mathrm{LF}}(s'+\mathrm{i}kV,k). \tag{19}$$

Note that if $u_+=0$ (as in the case of a homogeneous material) the product, μu_+, must be treated as the crack continuation stress, σ_+. In this case, Eq. (18) can be rewritten as

$$-U^{\mathrm{LF}}(s'+\mathrm{i}kv,k)\sigma_++u_-=U^{\mathrm{LF}}(s'+\mathrm{i}kV,k)q_-. \tag{20}$$

Also note that the function $f(s'+\mathrm{i}kV,k)$ in (12) has the same sense as $U^{\mathrm{LF}}(s'+\mathrm{i}kV,k)$ in (19). Recall that for the lattice we use the system of units where $\mu=1$.

Some important features of the fundamental solutions, $U^{\mathrm{LF}}(s'+\mathrm{i}kV,k)$ and $L(s'+\mathrm{i}kv,k)$ are discussed below.

Theorem on the fundamental solutions. *If* $s'>0$ (a) *the fundamental solution* $U^{\mathrm{LF}}(s'+\mathrm{i}kV,k)$ *cannot be positive and* (b) $kV\Im U^{\mathrm{LF}}(s'+\mathrm{i}kV,k)>0$ *if* $\Re U^{\mathrm{LF}}(s'+\mathrm{i}kV,k)>0$.

Correspondingly, if $s'>0$ (a') *the crack-related fundamental solution* $L(s'+\mathrm{i}kV,k)$ *cannot be zero or negative,* (b') $kV\Im L(s'+\mathrm{i}kV,k)<0$ *if* $\Re L^{\mathrm{LF}}(s'+\mathrm{i}kV,k)]<0$, (c') *on the real* k*-axis* $L(s'+\mathrm{i}kV,k)$ *and* $1/L(s'+\mathrm{i}kV,k)$ *are regular functions of* s'; *for* $s'=+0$ (d') $kV\Im L(0+\mathrm{i}kV,k)\leqslant 0$.

To prove the theorem consider the energy flux produced by the load

$$q_f=q_0\exp(s_0t-\mathrm{i}k_0\eta),\quad q_f^{\mathrm{F}}=2\pi\exp(s_0t)q_0\delta(k-k_0). \tag{21}$$

In this case

$$u^{\mathrm{F}}(k) = U^{\mathrm{LF}}(s_0 + \mathrm{i}kV, k)2\pi \exp(s_0 t) q_0 \delta(k - k_0) \tag{22}$$

and

$$u(t, \eta + Vt) = U^{\mathrm{LF}}(s_0 + \mathrm{i}k_0 V, k_0) q_0 \exp(s_0 t - \mathrm{i}k_0 \eta). \tag{23}$$

If one takes into account the work by both the real and the imaginary parts of the load, the energy flux, N, can be expressed as

$$\begin{aligned} N &= -\Re\left(\frac{\mathrm{d}u}{\mathrm{d}t}\bar{q}\right) = -|q_0|^2 \exp(2s_0 t)\Re[(s_0 + \mathrm{i}kV)U^{\mathrm{LF}}(s_0 + \mathrm{i}k_0 V, k_0)] \\ &= -|q_0|^2 \exp(2s_0 t)[s_0 \Re U^{\mathrm{LF}}(s_0 + \mathrm{i}k_0 V, k_0) - kV\Im U^{\mathrm{LF}}(s_0 + \mathrm{i}k_0 V, k_0)]. \end{aligned} \tag{24}$$

Because of passivity of the material, the energy flux cannot be directed from the half-plane, that is it cannot be negative. Statements $(a), (b)$ and $(a'), (b')$ and (d') of the theorem follow directly from the last relation. The regularity of L and $1/L$ [as in the statement (c')] follows directly from the regularity of U^{LF}.

The theorem is proved. □

Consider now what is the index of the fundamental solution $L(0 + \mathrm{i}kV, k)$ which is defined for $V > 0$ as

$$\mathrm{Ind}\, L(0 + \mathrm{i}kV, k) = \frac{1}{2\pi}[\mathrm{Arg}\, L(0 - \mathrm{i}\infty, -\mathrm{i}\infty) - \mathrm{Arg}\, L(0 + \mathrm{i}\infty, \mathrm{i}\infty)]. \tag{25}$$

Theorem on the index. *For* $V > 0$, *in a general case*, $-1 \leqslant \mathrm{Ind}\, L(0 + \mathrm{i}kV, k) \leqslant 0$, *while for the discrete lattice* (a) $L = 1$ $(k = \pm\infty)$ *and* (b) $\mathrm{Ind}\, L(0 + \mathrm{i}kV, k) = 0$.

The statement for a general case follows directly from the theorem on the fundamental solutions. Indeed, in the limit, $s = +0$, for negative k the function is above the real axis of the complex plane or on the positive half-axis; then it goes on to the negative half-plane or remains on the real axis. So, its trace on the complex plane can make not more than one clockwise revolution around the origin and hence the argument can be changed no more than from π to $-\pi$.

For the lattice, due to the presence of rigid particles, $f(s' + \mathrm{i}kV, k) \to 0$ if $s + \mathrm{i}kV \to \infty$ $[f = \mathrm{O}(1/(s + \mathrm{i}kV)^2]$. So, $L(s' + \mathrm{i}kV, k) \to 1$ $(s' \to \infty)$ and $L(s' + \mathrm{i}kV, k) = 1$ $(k = \pm\infty)$. It follows that $\mathrm{Ind}\, L = 0$ for large s' since its trace is a closed curve with the origin in the external domain. However, since the function $L(s' + \mathrm{i}kV, k)$ has neither singular nor zero points in the right half-plane of s', this equality is true for any positive s' and in the limit $s' = +0$.

The theorem is proved. These conclusions will be used in the factorization of L, in the determination of its long-wave asymptotes and in the calculations where $\mathrm{Arg}\, L$ is needed. □

3. Equations and general solutions

3.1. Dynamic equations

The dynamic equation for a particle outside the crack is

$$\frac{\mathrm{d}^2\boldsymbol{u}(t,\boldsymbol{x}')}{\mathrm{d}t^2}-\sum_{p=0}^{5}Q_p(t,\boldsymbol{x}')\boldsymbol{I}_p=0, \tag{26}$$

where $\boldsymbol{u}(t,\boldsymbol{x}')$ is the displacement vector and $Q_p(t,\boldsymbol{x}')$ is the elongation of the bond associated with vector $\boldsymbol{I}_p$:

$$Q_p(t,\boldsymbol{x}')=[\boldsymbol{u}(t,\boldsymbol{x}'+\boldsymbol{I}_p)-\boldsymbol{u}(t,\boldsymbol{x}')]\boldsymbol{I}_p. \tag{27}$$

For the considered steady-state problem, the displacements are assumed to depend on $\eta=x-Vt$ and y, that is $\boldsymbol{u}=\boldsymbol{u}(t,\boldsymbol{x})$, where $\boldsymbol{x}=\boldsymbol{x}'-(Vt+n/2)\boldsymbol{I}_0=(\eta,y)$. The equation of motion becomes

$$V^2\frac{\mathrm{d}^2\boldsymbol{u}(\boldsymbol{x})}{\mathrm{d}\eta^2}-\sum_{p=0}^{5}Q_p(\boldsymbol{x})\boldsymbol{I}_p=0,$$

$$Q_p(\boldsymbol{x})=[\boldsymbol{u}(\boldsymbol{x}+\boldsymbol{I}_p)-\boldsymbol{u}(\boldsymbol{x})]\boldsymbol{I}_p. \tag{28}$$

Denote projections of the displacements onto the x-, y-axis as $u_x(\eta,n),u_y(\eta,n)$. Accordingly, the elongation Q_p is $Q_p(\eta,n)$. In terms of the projections, Eq. (28) yields

$$V^2\frac{\mathrm{d}^2u_x}{\mathrm{d}\eta^2}-Q_0+Q_3-\frac{1}{2}(Q_1-Q_2-Q_4+Q_5)=0,$$

$$V^2\frac{\mathrm{d}^2u_y}{\mathrm{d}\eta^2}-\frac{\sqrt{3}}{2}(Q_1+Q_2-Q_4-Q_5)=0, \tag{29}$$

where

$$Q_0=u_x(\eta+1,n)-u_x(\eta,n),$$

$$Q_1=\tfrac{1}{2}[u_x(\eta+1/2,n+1)-u_x(\eta,n)]+\tfrac{\sqrt{3}}{2}[u_y(\eta+1/2,n+1)-u_y(\eta,n)],$$

$$Q_2=-\tfrac{1}{2}[u_x(\eta-1/2,n+1)-u_x(\eta,n)]+\tfrac{\sqrt{3}}{2}[u_y(\eta-1/2,n+1)-u_y(\eta,n)],$$

$$Q_3=-[u_x(\eta-1,n)-u_x(\eta,n)],$$

$$Q_4=-\tfrac{1}{2}[u_x(\eta-1/2,n-1)-u_x(\eta,n)]-\tfrac{\sqrt{3}}{2}[u_y(\eta-1/2,n-1)-u_y(\eta,n)],$$

$$Q_5=\tfrac{1}{2}[u_x(\eta+1/2,n-1)-u_x(\eta,n)]-\tfrac{\sqrt{3}}{2}[u_y(\eta+1/2,n-1)-u_y(\eta,n)]. \tag{30}$$

We now use the Fourier transform with respect to η. Eqs. (29) and expressions (30) in the transformed form are

$$Yu_x^{\mathrm{F}}-Q_0^{\mathrm{F}}+Q_3^{\mathrm{F}}-\tfrac{1}{2}(Q_1^{\mathrm{F}}-Q_2^{\mathrm{F}}-Q_4^{\mathrm{F}}+Q_5^{\mathrm{F}})=0,$$

$$Yu_y^{\mathrm{F}}-\tfrac{\sqrt{3}}{2}(Q_1^{\mathrm{F}}+Q_2^{\mathrm{F}}-Q_4^{\mathrm{F}}-Q_5^{\mathrm{F}})=0,$$

$$Y=(0+\mathrm{i}kV)^2,\qquad 0+\mathrm{i}kV=\lim(s'+\mathrm{i}kV)\quad(s'\to 0,\ \Re s'>0) \tag{31}$$

with

$$
\begin{aligned}
Q_0^{\mathrm{F}} &= (\mathrm{e}^{-\mathrm{i}k}-1)u_x^{\mathrm{F}}(k,n),\\
Q_1^{\mathrm{F}} &= \tfrac{1}{2}[u_x^{\mathrm{F}}(k,n+1)\mathrm{e}^{-\mathrm{i}k/2}-u_x^{\mathrm{F}}(k,n)]+\tfrac{\sqrt{3}}{2}[u_y^{\mathrm{F}}(k,n+1)\mathrm{e}^{-\mathrm{i}k/2}-u_y^{\mathrm{F}}(k,n)],\\
Q_2^{\mathrm{F}} &= -\tfrac{1}{2}[u_x^{\mathrm{F}}(k,n+1)\mathrm{e}^{\mathrm{i}k/2}-u_x^{\mathrm{F}}(k,n)]+\tfrac{\sqrt{3}}{2}[u_y^{\mathrm{F}}(k,n+1)\mathrm{e}^{\mathrm{i}k/2}-u_y^{\mathrm{F}}(k,n)],\\
Q_3^{\mathrm{F}} &= -(\mathrm{e}^{\mathrm{i}k}-1)u_x^{\mathrm{F}}(k,n),\\
Q_4^{\mathrm{F}} &= -\tfrac{1}{2}[u_x^{\mathrm{F}}(k,n-1)\mathrm{e}^{\mathrm{i}k/2}-u_x^{\mathrm{F}}(k,n)]-\tfrac{\sqrt{3}}{2}[u_y^{\mathrm{F}}(k,n-1)\mathrm{e}^{\mathrm{i}k/2}-u_y^{\mathrm{F}}(k,n)],\\
Q_5^{\mathrm{F}} &= \tfrac{1}{2}[u_x^{\mathrm{F}}(k,n-1)\mathrm{e}^{-\mathrm{i}k/2}-u_x^{\mathrm{F}}(k,n)]-\tfrac{\sqrt{3}}{2}[u_y^{\mathrm{F}}(k,n-1)\mathrm{e}^{-\mathrm{i}k/2}-u_y^{\mathrm{F}}(k,n)].
\end{aligned}
\tag{32}
$$

This results in the following equations:

$$
\begin{aligned}
&2(3-2\cos k+Y)u_x^{\mathrm{F}}(k,n)-\cos k/2[u_x^{\mathrm{F}}(k,n+1)+u_x^{\mathrm{F}}(k,n-1)]\\
&\quad+\sqrt{3}\mathrm{i}\sin k/2[u_y^{\mathrm{F}}(k,n+1)-u_y^{\mathrm{F}}(k,n-1)]=0\\
&-\sqrt{3}\mathrm{i}\sin k/2[u_x^{\mathrm{F}}(k,n+1)-u_x^{\mathrm{F}}(k,n-1)]\\
&\quad+3\cos k/2[u_y^{\mathrm{F}}(k,n+1)+u_y^{\mathrm{F}}(k,n-1)]-2(3+Y)u_y^{\mathrm{F}}(k,n)=0.
\end{aligned}
\tag{33}
$$

3.2. General solution for the intact lattice

Eqs. (33) are satisfied by the general solution

$$
u_x^{\mathrm{F}}(k,n)=C_x\lambda^n,\qquad u_y^{\mathrm{F}}(k,n)=C_y\lambda^n,
\tag{34}
$$

where C_x and C_y are independent of n. This yields equations regarding the constants

$$
\begin{aligned}
&[2(3-2\cos k+Y)-\cos k/2(\lambda+1/\lambda)]C_x+\sqrt{3}\mathrm{i}\sin k/2(\lambda-1/\lambda)C_y=0,\\
&-\sqrt{3}\mathrm{i}\sin k/2(\lambda-1/\lambda)C_x+[3\cos k/2(\lambda+1/\lambda)-2(3+Y)]C_y=0
\end{aligned}
\tag{35}
$$

and then an equation regarding λ

$$
\begin{aligned}
&(\lambda+1/\lambda)^2-2(4-2\cos k+\tfrac{4}{3}Y)\cos k/2(\lambda+1/\lambda)\\
&\quad+2(5-3\cos k)+\tfrac{4}{3}Y(6-2\cos k+Y)=0.
\end{aligned}
\tag{36}
$$

There are four roots:

$$
\begin{aligned}
&\lambda=\lambda_{1,2},\quad (|\lambda_{1,2}|<1 \text{ if } s'>0)\quad\text{and}\quad \lambda=\lambda_{3,4}=1/\lambda_{1,2};\\
&\qquad\lambda_{1,2}+1/\lambda_{1,2}=2n_{1,2},\quad \lambda_{1,2}=n_{1,2}-\sqrt{n_{1,2}^2-1},\\
&n_1=h_0-\sqrt{h_0^2-b},\quad n_2=h_0+\sqrt{h_0^2-b},\\
&h_0=(1+2\sin^2 k/2+\tfrac{2}{3}Y)\cos k/2,
\end{aligned}
$$

$$b = 1 + 3\sin^2 k/2 + \tfrac{1}{3}Y(4 + 4\sin^2 k/2 + Y),$$

$$h_0^2 - b = \frac{1}{9}Y^2 - 4\sin^2\frac{k}{2}\left(\sin^2\frac{k}{2} + \frac{1}{3}Y\right)^2. \tag{37}$$

Note that the sign of the square root in the expression for $\lambda_{1,2}$ is defined by the requirement: $|\lambda_{1,2}| < 1$. The sign shown in (37) corresponds, in particular, to real $n_{1,2}$ with $|n_{1,2}| > 1$. In the case where $|\lambda_{1,2}| = 1$ independently of the sign, as for instance, for real $n_{1,2}$ with $|n_{1,2}| < 1$, the sign can be determined using continuity of the functions when $s' > 0$. From the physical point of view these formal requirements correspond to a condition regarding the energy flux in the y-direction: it must be zero or positive at least if $s' > 0$.

The displacements for $n \geqslant 0$ can now be represented as

$$u_x^{\mathrm{F}}(k,n) = C_{x1}\lambda_1^n + C_{x2}\lambda_2^n,$$

$$u_y^{\mathrm{F}}(k,n) = C_{y1}\lambda_1^n + C_{y2}\lambda_2^n \tag{38}$$

with the equations for the coefficients:

$$f_x(\lambda_1)C_{x1} + f_y(\lambda_1)C_{y1} = 0,$$

$$f_x(\lambda_2)C_{x2} + f_y(\lambda_2)C_{y2} = 0, \tag{39}$$

where, as it follows from (35),

$$f_x(\lambda) = -\sqrt{3}\mathrm{i}\sin k/2(\lambda - 1/\lambda),$$

$$f_y(\lambda) = 3\cos k/2(\lambda + 1/\lambda) - 2(3 + Y). \tag{40}$$

Thus,

$$C_{y1} = g_1 C_{x1}, \quad g_1 = -\frac{f_x(\lambda_1)}{f_y(\lambda_1)},$$

$$C_{y2} = g_2 C_{x2}, \quad g_2 = -\frac{f_x(\lambda_2)}{f_y(\lambda_2)}. \tag{41}$$

3.3. Symmetry and the modes

To find the forces acting on particles with $n = 0$ ahead the crack, one has a need in expressions for the displacements at the lower crack face, $n = -1$, as well as for $n = 0$ (38). Consider two possibilities:

$$u_x(\eta,-1) = u_x(\eta,0),$$

$$u_y(\eta,-1) = -u_y(\eta,0) \tag{42}$$

and

$$u_x(\eta,-1) = -u_x(\eta,0),$$

$$u_y(\eta,-1) = u_y(\eta,0). \tag{43}$$

Due to symmetry of the lattice, a solution for the upper lattice half-plane with the continuity conditions (42), if it exists, can be continued to the lower half-plane as mode I:

$$u_x(\eta,-n-1)=u_x(\eta,n),$$
$$u_y(\eta,-n-1)=-u_y(\eta,n), \tag{44}$$

while the conditions of another type (43) lead to the continuation as mode II:

$$u_x(\eta,-n-1)=-u_x(\eta,n),$$
$$u_y(\eta,-n-1)=u_y(\eta,n). \tag{45}$$

In these cases, the displacements at $n\leqslant -1$, contrary to those for $n\geqslant 0$ (38), have the following expressions:

$$u_x^{\mathrm{F}}(k,n)=\pm C_{x1}\lambda_1^{-n-1}\pm C_{x2}\lambda_2^{-n-1},$$
$$u_y^{\mathrm{F}}(k,n)=\mp C_{y1}\lambda_1^{-n-1}\mp C_{y2}\lambda_2^{-n-1}. \tag{46}$$

Here and below, the upper and lower signs correspond to the modes I and II, respectively. From these conditions of symmetry and Eqs. (30) it follows that

$$Q_0(\eta,-1)=\pm Q_0(\eta,0),$$
$$Q_5(\eta,0)=\pm Q_4(\eta+\tfrac{1}{2},0), \tag{47}$$

where

$$Q_4(\eta,0)=\tfrac{1}{2}[u_x(\eta,0)\mp u_x(\eta-1/2,0)]+\tfrac{\sqrt{3}}{2}[u_y(\eta,0)\pm u_y(\eta-1/2,0)]$$
$$Q_4^{\mathrm{F}}(k,0)=\tfrac{1}{2}(1\mp \mathrm{e}^{\mathrm{i}k/2})u_x^{\mathrm{F}}(k,0)+\tfrac{\sqrt{3}}{2}(1\pm \mathrm{e}^{\mathrm{i}k/2})u_y^{\mathrm{F}}(k,0),$$
$$Q_5^{\mathrm{F}}(k,0)=\pm Q_4^{\mathrm{F}}(k,0)\mathrm{e}^{-\mathrm{i}k/2}. \tag{48}$$

3.4. Dynamic equation for a particle with $n=0$

Now consider equations of motion for a particle on the line $n=0$. They differ from Eq. (31) by the expressions for Q_4^{F} and Q_5^{F}. Indeed, in Eq. (31) these values represent forces acting on the particle only ahead the crack, and we denote $Q_4^{\mathrm{F}}=Q_+$, while Q_5 is defined by Eq. (48). Note that subscript '+' denotes the right-side Fourier transform, while subscript '−' is used for the left-side Fourier transform. In addition to the internal forces, we introduce external forces, $q_4=q(\eta)$ and $q_5(\eta)=\pm q(\eta+1/2)$ directed as Q_4 and Q_5, respectively (as was already noted, these forces are introduced for convenience in an initial stage of the considerations).

So, for $n=0$ we have

$$Yu_x^{\mathrm{F}}(k,0)-Q_0^{\mathrm{F}}-\tfrac{1}{2}Q_1^{\mathrm{F}}+\tfrac{1}{2}Q_2^{\mathrm{F}}+Q_3^{\mathrm{F}}=-\tfrac{1}{2}(1\mp \mathrm{e}^{-\mathrm{i}k/2})(Q_++q^{\mathrm{F}}),$$
$$Yu_y^{\mathrm{F}}(k,0)-\tfrac{\sqrt{3}}{2}(Q_1^{\mathrm{F}}+Q_2^{\mathrm{F}})=-\tfrac{\sqrt{3}}{2}(1\pm \mathrm{e}^{-\mathrm{i}k/2})(Q_++q^{\mathrm{F}}). \tag{49}$$

These equations can be simplified taking into account Eqs. (31) considered with their 'analytical continuation' to include the crack surface, $n=0$. These relations allow one to express the left-hand sides of Eqs. (49) in terms of Q_4 and Q_5 which correspond to the analytical continuation (but not the considered symmetry!). To avoid confusion we denote them ${}^*Q_4$ and ${}^*Q_5$. As a result we get

$$
\begin{aligned}
&{}^*Q_5^{\mathrm{F}} - {}^* Q_4^{\mathrm{F}} = (1 \mp \mathrm{e}^{-\mathrm{i}k/2})(Q_+ + q^{\mathrm{F}}),\\
&{}^*Q_5^{\mathrm{F}} + {}^* Q_4^{\mathrm{F}} = (1 \pm \mathrm{e}^{-\mathrm{i}k/2})(Q_+ + q^{\mathrm{F}}),
\end{aligned}
\tag{50}
$$

where, in accordance with expressions (32),

$$
\begin{aligned}
{}^*Q_4^{\mathrm{F}} &= -\tfrac{1}{2}[(C_{x1}\lambda_1^{-1} + C_{x2}\lambda_2^{-1})\mathrm{e}^{\mathrm{i}k/2} - C_{x1} - C_{x2}]\\
&\quad - \tfrac{\sqrt{3}}{2}[(C_{x1}g_1\lambda_1^{-1} + C_{x2}g_2\lambda_2^{-1})\mathrm{e}^{\mathrm{i}k/2} - C_{x1}g_1 - C_{x2}g_2],\\
{}^*Q_5^{\mathrm{F}} &= \tfrac{1}{2}[(C_{x1}\lambda_1^{-1} + C_{x2}\lambda_2^{-1})\mathrm{e}^{-\mathrm{i}k/2} - C_{x1} - C_{x2}]\\
&\quad - \tfrac{\sqrt{3}}{2}[(C_{x1}g_1\lambda_1^{-1} + C_{x2}g_2\lambda_2^{-1})\mathrm{e}^{-\mathrm{i}k/2} - C_{x1}g_1 - C_{x2}g_2].
\end{aligned}
\tag{51}
$$

It follows that

$$
\begin{aligned}
&\left(\frac{1}{\lambda_1}\cos\frac{k}{2} - 1 + \mathrm{i}\sqrt{3}\,\frac{g_1}{\lambda_1}\sin\frac{k}{2}\right)C_{x1} + \left(\frac{1}{\lambda_2}\cos\frac{k}{2} - 1 + \mathrm{i}\sqrt{3}\,\frac{g_2}{\lambda_2}\sin\frac{k}{2}\right)C_{x2}\\
&\quad = (1 \mp \mathrm{e}^{-\mathrm{i}k/2})(Q_+ + q^{\mathrm{F}}),\\
&\left(\frac{\mathrm{i}}{\lambda_1}\sin\frac{k}{2}\sqrt{3}g_1\left(\frac{1}{\lambda_1}\cos\frac{k}{2} - 1\right)\right)C_{x1} + \left(\frac{\mathrm{i}}{\lambda_2}\sin\frac{k}{2}\sqrt{3}g_2\left(\frac{1}{\lambda_2}\cos\frac{k}{2} - 1\right)\right)C_{x2}\\
&\quad = -(1 \pm \mathrm{e}^{-\mathrm{i}k/2})(Q_+ + q^{\mathrm{F}}).
\end{aligned}
\tag{52}
$$

These equations allow one to obtain the coefficients, C_{x1} and C_{x2}, then–C_{y1} and C_{y2} (41), further—the displacements at $n=0$ (38) and $n=-1$ (see Eqs. (44) or (45)) and at last—an expression for Q_4^{F} (48) in terms of $Q_4 + q^{\mathrm{F}}$.

3.5. Green function L and dispersion relations

3.5.1. Crack-related fundamental solution

Based on the dependence for $Q_4^{\mathrm{F}} \equiv Q_+ + Q_-$ the governing equation (11) can be obtained with

$$
L(0 + \mathrm{i}kV, k) = \frac{r_\Delta}{h_\Delta},
\tag{53}
$$

$$
\begin{aligned}
&r_\Delta = 3\sqrt{n_1^2 - 1}\sqrt{n_2^2 - 1},\\
&h_\Delta = \frac{F(n_2)\sqrt{n_1^2 - 1} - F(n_1)\sqrt{n_2^2 - 1}}{n_2 - n_1},\\
&F(n_{1,2}) = 3(\cos k/2 - n_{1,2})^2 + 6\sin^2 k/2(1 \pm \cos k/2)(1 \mp n_{1,2})\\
&\qquad + Y[(1 \pm \cos k/2)(1 \mp n_{1,2}) + 1 - n_{1,2}\cos k/2].
\end{aligned}
\tag{54}
$$

3.5.2. Dispersion relations

Consider a free intact lattice. In this case, we have to introduce the *force* Q^{F} instead Q_+ in the right-hand side of Eq. (10). For free lattice, $q=0$, this leads to the equation

$$L(0+\mathrm{i}kV,k)Q^{\mathrm{F}}(k)=0. \tag{55}$$

Real zeros of L thus correspond to free waves in the intact lattice under the conditions of symmetry, Eq. (42) or Eq. (43). Along with this, as will be seen below, such waves appear in the problem under consideration. The equation $r_\Delta=0$ is satisfied by four dispersion relations $\Omega=\Omega(k)$, where $\Omega=kV$ is the frequency of the sinusoidal wave, $\exp(-\mathrm{i}k\eta)=\exp[\mathrm{i}(\Omega t-kx)]$. The first is

$$\Omega=\Omega_1=[3-\cos(k/2)-2\cos(k)]^{1/2},$$
$$n_2=1,\quad n_1=-1-\tfrac{2}{3}\cos(k/2)\,[1-2\cos(k/2)-2\cos^2(k/2)]. \tag{56}$$

For $k\to 0$, that is in the long-wave approximation, this dispersion relation corresponds to a plane longitudinal wave. Indeed, in this case, $V=\Omega/k\sim c_1=\sqrt{9/8}$ (see Section 2.1). Then,

$$\Omega=\Omega_2=\sqrt{6}\,|\sin(k/4)|,$$
$$n_2=1,\quad n_1=1+4\sin^2(k/4)[1-8\sin^2(k/4)+8\sin^4(k/4)]. \tag{57}$$

This relation corresponds to a plane shear wave: $V\sim c_2=\sqrt{3/8}$ $(k\to 0)$. Further,

$$\Omega=\Omega_3=\sqrt{6}\,|\cos(k/4)|,$$
$$n_1=-1,\quad n_2=-1-4\cos^2(k/4)[1-8\cos^2(k/4)+8\cos^4(k/4)]. \tag{58}$$

Lastly,

$$\Omega=\Omega_4=[2\cos^2(k/4)+4\sin^2(k/2)]^{1/2},$$
$$n_1=-1,\quad n_2=-1+\tfrac{4}{3}\cos^2(k/4)[9-16\cos^2(k/4)+8\cos^4(k/4)]. \tag{59}$$

The last two relations have no analogue on the macrolevel.

Now consider a free lattice half-plane, that is Eq. (10) with $Q_+=q^{\mathrm{F}}=0$ in the right-hand side. In this case, a nontrivial solution can exist if $1/f(0+\mathrm{i}kV,k)=0$, that is $1/L(0+\mathrm{i}kV,k)=0$. The equation $h_\Delta=0$, where h_Δ is different for different modes, is satisfied by the dispersion relation

$$\Omega=\Omega_{\mathrm{R}}=(3-\sqrt{3})^{1/2}\,|\sin(k/2)|, \tag{60}$$

valid for each mode. It corresponds to the lattice Rayleigh wave. Besides, relations (57) and (59) are valid for mode I and relations (56) and (58)—for mode II. These zeros of r_Δ and h_Δ cancel each other (it can be shown that they are each of the first order). Thus there are three dispersion relations for mode I:

$$\Omega_{\mathrm{R}}=(3-\sqrt{3})^{1/2}|\sin(k/2)|\quad(h_\Delta=0),$$
$$\Omega_1=[3-\cos(k/2)-2\cos(k)]^{1/2}\quad(r_\Delta=0),$$
$$\Omega_3=\sqrt{6}\,|\cos(k/4)|\quad(r_\Delta=0) \tag{61}$$

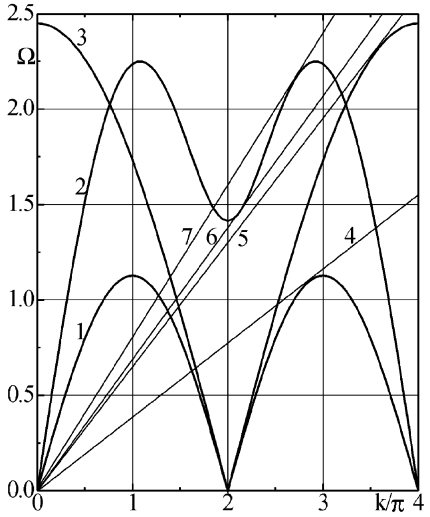

Fig. 2. Dispersion relations for mode I (61): (1) the lattice Rayleigh wave; (2) the lattice longitudinal wave; (3) the optical-I wave. The resonant rays: (4) $V \approx 0.122k$; (5) $V \approx 0.207k$; (6) $V \approx 0.218k$; (7) $V \approx 0.254k$.

shown in Fig. 2, and three dispersion relations for mode II:

$$\Omega_{\mathrm{R}} = (3-\sqrt{3})^{1/2}|\sin(k/2)| \quad (h_{\Delta}=0),$$

$$\Omega_2 = \sqrt{6}|\sin(k/4)| \quad (r_{\Delta}=0),$$

$$\Omega_4 = [2\cos^2(k/4) + 4\sin^2(k/2)]^{1/2} \quad (r_{\Delta}=0) \tag{62}$$

shown in Fig. 3. Also, four 'resonant' rays are shown in Fig. 2, and two such rays—in Fig. 3. Note that all these dispersion relations are valid together with their periodic continuation: $\Omega(k+4\pi)=\Omega(k)$. This is a manifestation of the periodicity of the discrete lattice. For the determination of the bond elongation or the particle displacements, the continuation does not represent any additional information. However, it is useful for the determination of the waves excited by a moving source (the *dissipative waves*) or the waves with the energy release in the moving sink (the *feeding waves*). For such a wave, the wavenumber $k=\Omega/V$ is outside the 'main' region, $0 \leqslant k < 4\pi$, if the speed, V, is low enough.

For a long wave, that is for small k, relations Ω_{R}, Ω_1 and Ω_2 correspond to low frequency; they can be called the *acoustic branches*, while relations Ω_3 and Ω_4 correspond to high frequency of antiphase oscillations; they can be called the *optical branches*. Accordingly, we will call Ω_{R} the Rayleigh wave branch, Ω_1 and Ω_2—the longitudinal and shear wave branches, respectively, and Ω_3 and Ω_4—the optical-I and -II branches, respectively.

The dispersion relations are used below for the determination of possible configurations of the feeding and dissipative waves, while the functions $\lambda_{1,2}$, together with equalities (41) and (52), define the wave modes.

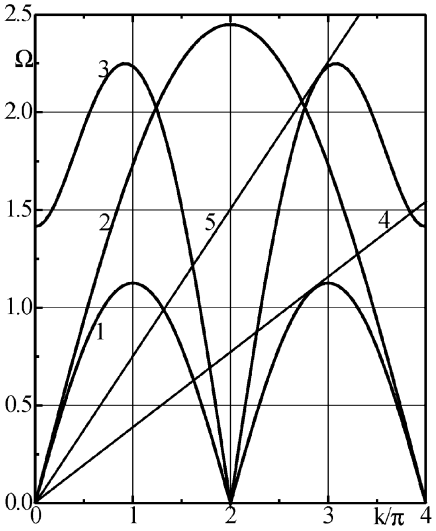

Fig. 3. Dispersion relations for mode II (62): (1) the lattice Rayleigh wave; (2) the lattice shear wave; (3) the optical-II wave; The resonant rays: (4) $V \approx 0.122k$; (5) $V \approx 0.239k$.

3.5.3. Wave modes

The dependences for $n_{1,2}$ and $\lambda_{1,2}$ are represented in Figs. 4 (for Ω_R), 5 (for Ω_1), 6 (for Ω_2), 7 (for Ω_3) and, at last, in Fig. 8 (for Ω_4). These dependences serve in the determination of the wave modes. For the lattice Rayleigh wave (Fig. 4(b)) $\lambda_{1,2} < 1$ (except points $k = 0, \pi, \ldots$) and the wave amplitude decreases exponentially as the distance from the surface increases. The other dispersion dependences correspond to the cases where $n_1^2 = 1$ or $n_2^2 = 1$. Accordingly, $\lambda_1^2 = 1$ or $\lambda_2^2 = 1$ (see Eqs. (37)). The corresponding part of the displacements is independent of y ($\lambda_1 = 1$ or $\lambda_2 = 1$) or represents an antiphase-oscillation solution ($\lambda_1 = -1$ or $\lambda_2 = -1$). Another part of the displacement (see Eq. (38)) represents a crack-path-associated solution vanishing with an increase of $|y|$ (the case $|\lambda| < 1$) or a constant-amplitude wave with a sinusoidal dependence on y.

3.6. General solution

The function $L(s' + \mathrm{i}kV, k)$ satisfies the conditions (see Section 2.3) which allow one to factorize it using the Cauchy-type integral:

$$L(s' + \mathrm{i}kV, k) = L_+(s' + \mathrm{i}kV, k) L_-(s' + \mathrm{i}kV, k),$$

$$L_\pm(s' + \mathrm{i}kV, k) = \exp\left(\pm \frac{1}{2\pi \mathrm{i}} \int_{-\infty}^{\infty} \frac{\ln L(s' + \mathrm{i}\xi V, \xi)}{\xi - k} \, \mathrm{d}\xi \right), \tag{63}$$

where $\Im k > 0$ for L_+, $\Im k < 0$ for L_- and $\operatorname{Arg} L(s' + \mathrm{i}\xi V, \xi) = 0$ ($\xi = \pm\infty$).

In this product, L_+ [L_-] is a regular function of k in the upper [lower] half-plane (including the real axis if $s' > 0$). In accordance with Appendix B of Part I (Slepyan,

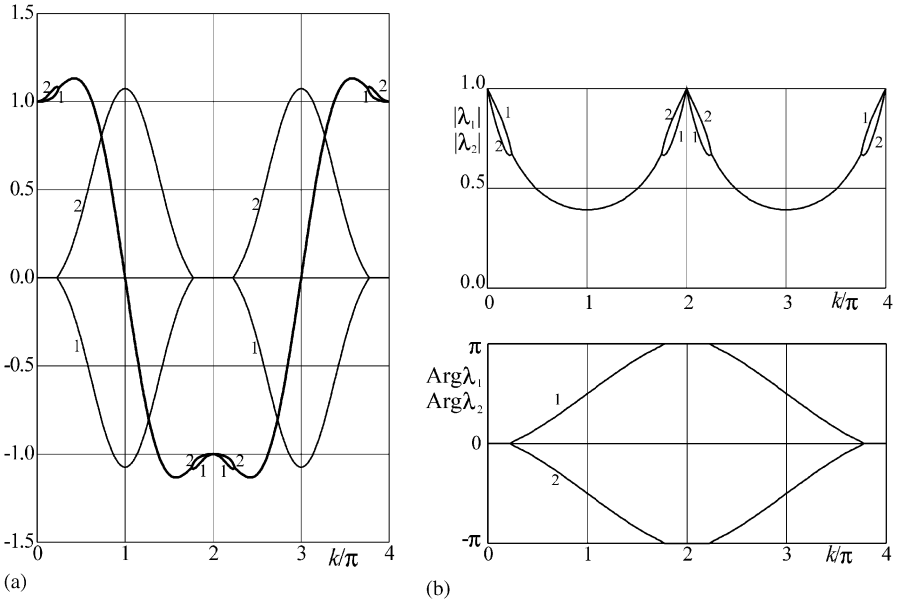

Fig. 4. The lattice Rayleigh wave: (a) (1) n_1; (2) n_2 (thick curves: $\Re n_{1,2}$, thin curves: $\Im(n_{1,2})$ and (b) (1) λ_1; (2) λ_2.

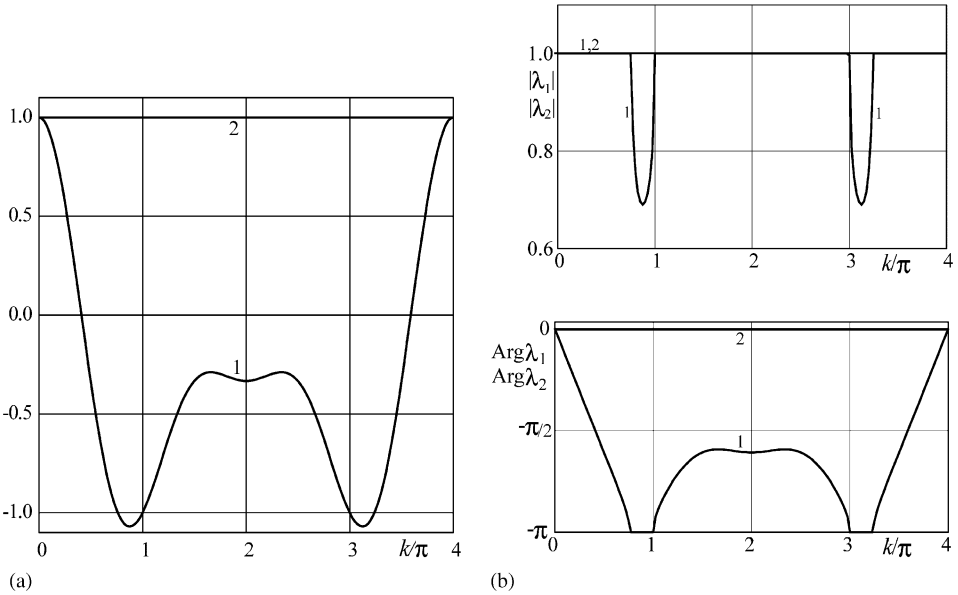

Fig. 5. The lattice longitudinal wave: (a) (1) n_1; (2) n_2 and (b) (1) λ_1; (2) λ_2.

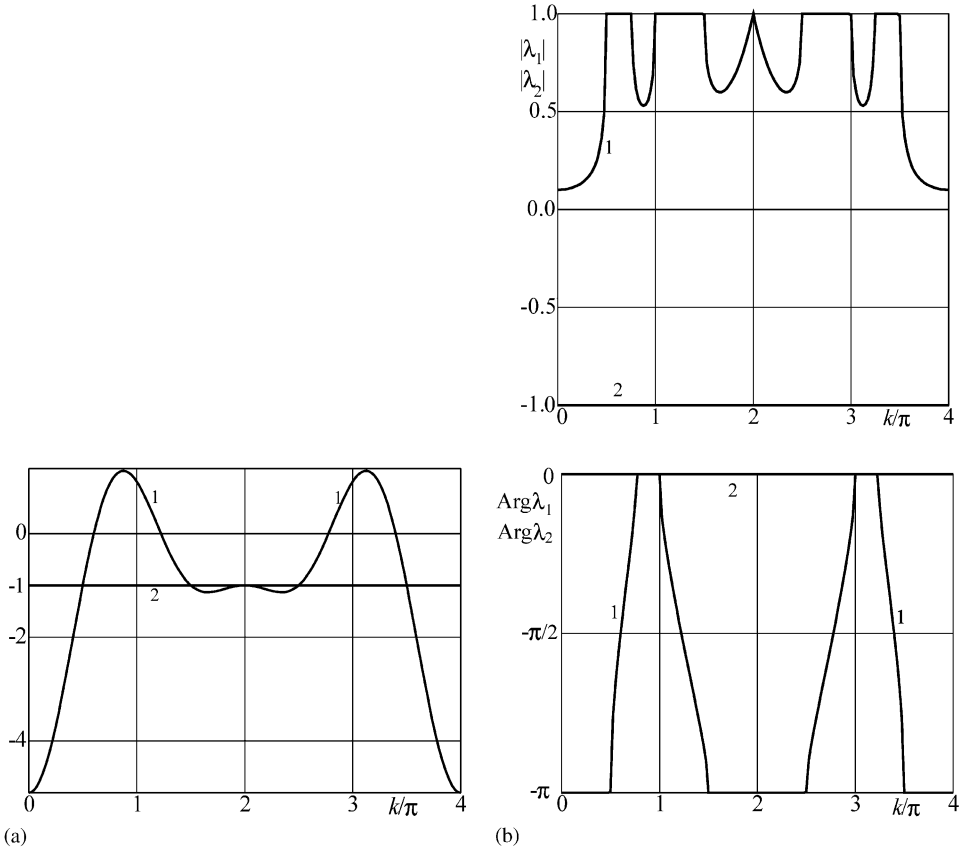

Fig. 6. The lattice shear wave: (a) (1) n_1; (2) n_2 and (b) (1) λ_1; (2) λ_2.

2001a), $L_+(0 + \mathrm{i}kV,k)[L_-(0 + \mathrm{i}kV,k)]$ incorporates singular and zero points of $L(0+\mathrm{i}kV,k)$, defined by the dispersion relations, Eqs. (61) and (62), where $V=\Omega/k < V_g=\mathrm{d}\Omega/\mathrm{d}k$ $[V > V_g]$. In the case $V=V_g$, the corresponding singular or zero point, as a double root split by the factorization, belongs to each of the functions $L_\pm$. Note that

$$\lim L_+(s' + \mathrm{i}kV,k)=1 \quad (k \to \mathrm{i}\infty), \qquad \lim L_-(s' + \mathrm{i}kV,k)=1 \quad (k \to -\mathrm{i}\infty). \tag{64}$$

The governing equation (11) can now be represented as

$$L_+(0 + \mathrm{i}kV,k)Q_+ + \frac{Q_-}{L_-(0 + \mathrm{i}kV,k)} = \left[\frac{1}{L_-(0 + \mathrm{i}kV,k)} - L_+(0 + \mathrm{i}kV,k)\right] q^{\mathrm{F}}. \tag{65}$$

In the following, we consider homogeneous solutions which correspond to $q(\eta)=0$ but with a nonzero right-hand side of Eq. (65). Note that the homogeneous equation (65) has only the trivial solution, $Q_+=Q_-=0$, as follows from the same consideration as

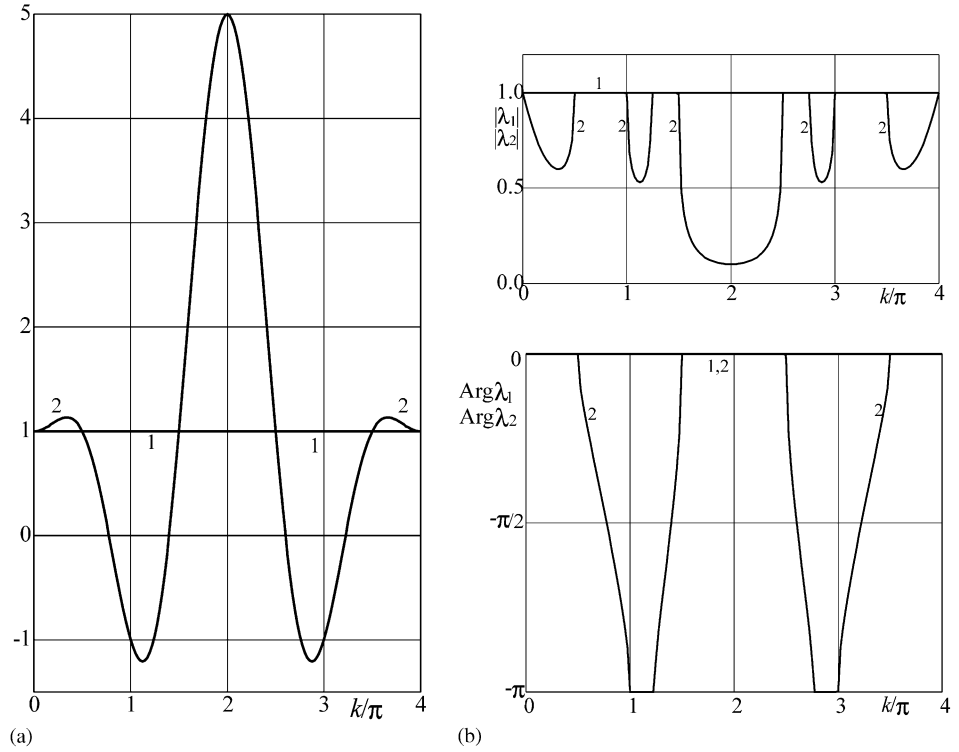

Fig. 7. The optical-I wave: (a) (1) n_1; (2) n_2 and (b) (1) λ_1; (2) λ_2.

in part I (Slepyan, 2001a). To obtain a nontrivial solution we consider nonzero q^{F}, such that $q^{\mathrm{F}} \to 0$ with a nonzero limit of the right-hand side of Eq. (65). We consider a regular case, $V \neq V_g$.

Let h_+ (h_-) be a real root of the equation $h_\Delta = 0$, such that for this wavenumber $V_g > V$ ($V_g < V$), and r_+ (r_-) be a real root of the equation $r_\Delta = 0$ where $V_g > V$ ($V_g < V$). Suppose that

$$L_+(s' + \mathrm{i}kV, k) \sim L_h[a_+ s' - \mathrm{i}(k - h_+)]^{-\nu} \quad (k \to h_+, s' \to +0),\ \nu > 0,$$

$$L_-(s' + \mathrm{i}kV, k) \sim L_r[a_- s' + \mathrm{i}(k - r_-)]^{\mu} \quad (k \to r_-, s' \to +0),\ \mu > 0. \tag{66}$$

where L_h, ν and L_r, μ are constants, $a_+ = 1/(V - V_g)$ ($V_g < V$) and $a_- = 1/(V_g - V)$ ($V < V_g$) (see Appendix B in Part I, Slepyan, 2001a).

Let us further take the external force as

$$q = -q_h(2a_+ s')^{\nu} \exp[(a_+ s' - \mathrm{i}h_+)\eta] H(-\eta) + q_r(2a_- s')^{\mu} \exp[-(a_- s' + \mathrm{i}r_-)\eta] H(\eta), \tag{67}$$

that is

$$q^{\mathrm{F}} = -\frac{(2a_+ s')^{\nu}}{a_+ s' + \mathrm{i}(k - h_+)} q_h + \frac{(2a_- s')^{\mu}}{a_- s' - \mathrm{i}(k - r_-)} q_r. \tag{68}$$

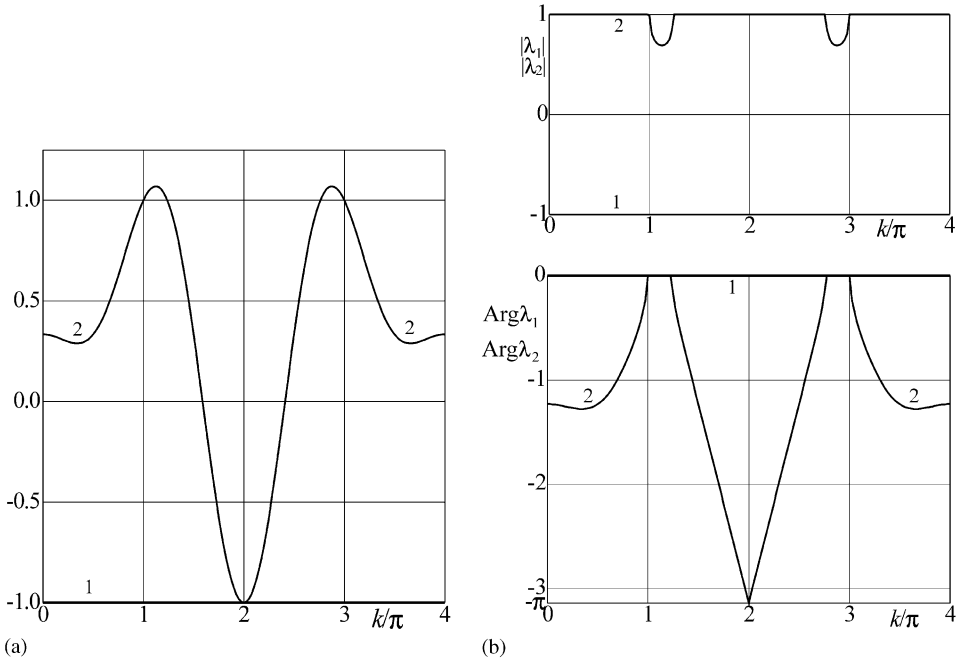

Fig. 8. The optical-II wave: (a) (1) n_1; (2) n_2 and (b) (1) λ_1; (2) λ_2.

So, the condition, $q \to 0$ with $s' \to 0$, is satisfied.

For $s' \to +0$ it follows (see Appendix C of part I (Slepyan, 2001a)) that

$$L_+Q_+ + \frac{Q_-}{L_-} \sim 2\pi\left[L_h q_h \delta(k-h_+) + \frac{q_r}{L_r}\delta(k-r_-)\right]$$
$$= L_h q_h\left[\frac{1}{0+\mathrm{i}(k-h_+)} + \frac{1}{0-\mathrm{i}(k-h_+)}\right] + \frac{q_r}{L_r}\left[\frac{1}{0+\mathrm{i}(k-r_-)} + \frac{1}{0-\mathrm{i}(k-r_-)}\right]. \tag{69}$$

Thus the solution is

$$Q_+ = \frac{1}{L_+(k)}\left[\frac{L_h q_h}{0-\mathrm{i}(k-h_+)} + \frac{q_r}{L_r}\frac{1}{0-\mathrm{i}(k-r_-)}\right],$$
$$Q_- = L_-(k)\left[\frac{L_h q_h}{0+\mathrm{i}(k-h_+)} + \frac{q_r}{L_r}\frac{1}{0+\mathrm{i}(k-r_-)}\right]. \tag{70}$$

The general solution can be represented as a sum over all the wavenumbers h_+ and r_- which correspond to the dispersion relations (61) (mode I) or (62) (mode II) under a given crack speed, V. Also, for each wavenumber, similar solutions corresponding to $k = -h_+$ and $k = -r_-$ should be taken into account to obtain real results.

Note that $Q_{\pm}$ consists of the first (the second) term only if only the first (the second) condition in Eq. (66) is satisfied, that is $v > 0$ ($\mu > 0$), and the homogeneous solution does not exist at all if neither one nor other condition is true.

4. Macrolevel-associated solution

We call a *macrolevel-associated solution* one that corresponds to a zero feeding wavenumber. To find such a solution we need asymptotes of the lattice relations for $k \to 0$.

4.1. Asymptotes of some relations

The asymptotes of the functions introduced in (37) are

$$h_0 \sim 1 + \tfrac{3}{8}k^2 + \tfrac{2}{3}Y - \tfrac{13}{128}k^4 - \tfrac{1}{12}Yk^2,$$

$$b \sim 1 + \tfrac{3}{4}k^2 + \tfrac{2}{3}Y - \tfrac{1}{16}k^4 + \tfrac{1}{3}Y(k^2 + Y),$$

$$h_0^2 - b \sim \tfrac{1}{9}Y^2 - \tfrac{1}{16}Yk^4 - \tfrac{1}{9}Y^2k^2, \tag{71}$$

where $Y = (0 + \mathrm{i}kV)^2$. It follows that

$$n_1 \sim 1 + \frac{3}{8}\alpha_1^2 + \frac{19}{128}k^4 + \frac{1}{12}Yk^2 + \frac{3k^6}{32Y},$$

$$n_2 \sim 1 + \frac{3}{8}\alpha_2^2 - \frac{45}{128}k^4 - \frac{1}{4}Yk^2 - \frac{3k^6}{32Y},$$

$$n_2 - n_1 \sim \frac{2}{3}Y,$$

$$\alpha_1 = \sqrt{k^2 + Y/c_1^2}, \qquad \alpha_2 = \sqrt{k^2 + Y/c_2^2}, \tag{72}$$

where $c_1^2 = 9/8$ and $c_2^2 = 3/8$ are velocities of long longitudinal and shear waves, respectively. Depending on the crack speed range the functions α_1 and α_2 are

$$\alpha_1 = \sqrt{1 - V^2/c_1^2}\sqrt{(0 + \mathrm{i}k)(0 - \mathrm{i}k)} \quad (0 \leqslant V < c_1),$$

$$\alpha_1 = \sqrt{V^2/c_1^2 - 1}(0 + \mathrm{i}k) \quad (c_1 < V),$$

$$\alpha_2 = \sqrt{1 - V^2/c_2^2}\sqrt{(0 + \mathrm{i}k)(0 - \mathrm{i}k)} \quad (0 \leqslant V < c_2),$$

$$\alpha_2 = \sqrt{V^2/c_2^2 - 1}(0 + \mathrm{i}k) \quad (c_2 < V). \tag{73}$$

Further,

$$\sqrt{n_1^2 - 1} \sim \tfrac{\sqrt{3}}{2}\alpha_1, \qquad \sqrt{n_2^2 - 1} \sim \tfrac{\sqrt{3}}{2}\alpha_2. \tag{74}$$

Note that for the determination of an asymptote of $L(0 + \mathrm{i}kV, k)$ different accuracy for different values in Eqs. (71)–(74) is required.

As to functions $\lambda_{\pm}$, the asymptotes, $k \to 0$, valid for any n (or y) follow from their definition:

$$\lambda_{1,2}^n = (n_{1,2} - \sqrt{n_{1,2}^2 - 1})^n \sim \exp(-\tfrac{\sqrt{3}}{2}\alpha_{1,2} n)$$

$$= \exp(-\alpha_{1,2} y) \quad (k \to 0, k^2 n \to 0, n \geqslant 0). \tag{75}$$

This yields

$$\lambda_{1,2} \sim \exp(-\tfrac{\sqrt{3}}{2}\alpha_{1,2}). \tag{76}$$

4.2. Asymptotes for L

An asymptote of L for $k \to 0$ corresponds to the classical description for an elastic homogeneous body with the above-mentioned nondimensional parameters, $\rho = 2/\sqrt{3}$, $c_1 = \sqrt{9/8}$ and $c_2 = \sqrt{3/8}$. For mode I we get

$$F(n_1) \sim -\tfrac{3}{32}(k^2 + \alpha_2^2)^2,$$

$$F(n_2) \sim -\tfrac{3}{8}\alpha_2^2 k^2 \tag{77}$$

and

$$L(0 + \mathrm{i}kV, k) = L_{\mathrm{I}} \sim L_{\mathrm{I}}^0 = \frac{32 Y \alpha_1}{\sqrt{3} R_0},$$

$$R_0 = (k^2 + \alpha_2^2)^2 - 4k^2 \alpha_1 \alpha_2, \tag{78}$$

while for mode II

$$F(n_1) \sim \tfrac{9}{8}\alpha_1^2 k^2,$$

$$F(n_2) \sim \tfrac{9}{32}(k^2 + \alpha_2^2)^2 \tag{79}$$

and

$$L(0 + \mathrm{i}kV, k) = L_{\mathrm{II}} \sim L_{\mathrm{II}}^0 = \frac{32 Y \alpha_2}{3\sqrt{3} R_0} \tag{80}$$

with the same expression for R_0 as for mode I (78). Note that the considered function, $L(0+\mathrm{i}kV, k)$, connects the elongation of an inclined bond (or its trace) on the crack path with external force of the same orientation. Referring to the corresponding continuous medium, one can express the crack opening displacement, and stresses on the crack continuation as follows:

$$u_y = Q/\sqrt{3} \text{ (mode I)}, \quad u_x = Q \text{ (mode II)},$$

$$\sigma_{yy} = \sqrt{3} q, \text{ (mode I)}, \quad \sigma_{yx} = q, \text{ (mode II)}. \tag{81}$$

We come to the classical relations

$$u_y^{\mathrm{F}} = \frac{1}{3} L_{\mathrm{I}}^0 \sigma_{yy}^{\mathrm{F}}, \quad \frac{1}{3} L_{\mathrm{I}}^0 = \frac{Y \alpha_1}{\rho c_2^4 R_0} \text{ (mode I)},$$

$$u_x^{\mathrm{F}} = L_{\mathrm{II}}^0 \sigma_{yx}^{\mathrm{F}}, \quad L_{\mathrm{II}}^0 = \frac{Y \alpha_2}{\rho c_2^4 R_0} \text{ (mode II)}. \tag{82}$$

Recall that for the considered lattice $\rho = 2/\sqrt{3}$ and $c_2^2 = 3/8$.

Below we use the following notations:

$$\beta_{1,2} = \sqrt{1 - V^2/c_{1,2}^2} \quad (V < c_{1,2}),$$

$$\beta_{1,2}^* = \sqrt{V^2/c_{1,2}^2 - 1} \quad (c_{1,2} < V),$$

$$R^0 = 4\beta_1\beta_2 - (1+\beta_2^2)^2, \quad R^0 > 0 \ (0 < V < c_R), \quad R^0 < 0 \ (c_R < V < c_2). \tag{83}$$

We also take into account that

$$\alpha_{1,2}^2 = [0 + ik(1 + V/c_{1,2})][0 - ik(1 - V/c_{1,2})],$$

$$k^2 + \alpha_2^2 = [0 + ik(\sqrt{2} + V/c_2)][0 - ik(\sqrt{2} - V/c_2)]. \tag{84}$$

Further, if one retraces the path on the complex plane of a function when k runs from $-\infty$ to ∞, it can be found that

$$\operatorname{Ind} Y = 1 \quad (0 < V),$$

$$\operatorname{Ind} \alpha_{1,2} = 0 \quad (0 < V < c_{1,2}), \qquad \operatorname{Ind} \alpha_{1,2} = 1 \quad (c_{1,2} < V),$$

$$\operatorname{Ind} R_0 = 1 \quad (0 < V < c_R), \qquad \operatorname{Ind} R_0 = 2 \quad (c_R < V < c_2, c_1 < V),$$

$$\operatorname{Ind} R_0 = \tfrac{3}{2} + \omega \quad (c_2 < V < c_1), \quad \omega = \frac{1}{\pi} \arctan \frac{(1+\beta_2^2)^2}{4\beta_1\beta_2^*},$$

$$c_R = \tfrac{1}{2}\sqrt{3 - \sqrt{3}}. \tag{85}$$

We can now write down the asymptotic expressions for $L(0 + ikV, k)$ $(\Omega, k \to 0)$ in different ranges of the crack speed.

Mode I:

In the range $0 < V < c_R$

$$L_I^0 = \frac{32V^2\beta_1}{\sqrt{3}R^0} \frac{1}{\sqrt{(0+ik)(0-ik)}} > 0. \tag{86}$$

In this range, $\operatorname{Arg} L_I = 0$ in a vicinity of $k = 0$ and it is a function of finite support.

In the range $c_R < V < c_2$, the considered function can be represented as

$$L_I^0 = -\frac{32V^2\beta_1}{\sqrt{3}R^0}(0 - ik)^{1/2}(0 + ik)^{-3/2}. \tag{87}$$

In the range $c_2 < V < c_1$, we can use the representation

$$L_I^0 = \frac{32V^2\beta_1}{\sqrt{3}T}(0 - ik)^{\omega}(0 + ik)^{-1-\omega}, \quad T = |R_0|. \tag{88}$$

Lastly, for $c_1 < V$

$$L_I^0 = \frac{32V^2\beta_1^*}{\sqrt{3}[4\beta_1^*\beta_2^* + (1+\beta_2^2)^2](0+ik)}. \tag{89}$$

For *mode* II:

$$L_{\rm II}^0 = \frac{32V^2\beta_2}{3\sqrt{3}R^0}\frac{1}{\sqrt{(0+{\rm i}k)(0-{\rm i}k)}} \quad (0 < V < c_{\rm R}), \tag{90}$$

$$L_{\rm II}^0 = -\frac{32V^2\beta_2}{3\sqrt{3}R^0}(0-{\rm i}k)^{1/2}(0+{\rm i}k)^{-3/2} \quad (c_{\rm R} < V < c_2), \tag{91}$$

$$L_{\rm II}^0 = \frac{32V^2\beta_2^*}{3\sqrt{3}T}(0-{\rm i}k)^{\omega-1/2}(0+{\rm i}k)^{-1/2-\omega} \quad (c_2 < V < c_1), \tag{92}$$

$$L_{\rm II}^0 = \frac{32V^2\beta_2^*}{3\sqrt{3}[4\beta_1^*\beta_2^* + (1+\beta_2^2)^2](0+{\rm i}k)} \quad (c_1 < V). \tag{93}$$

4.3. Asymptotes for $L_\pm$

4.3.1. Sub-Rayleigh speed

The long-wave/low-frequency approximation of the functions $L_\pm$ can be found using the Cauchy-type integral (63) and the asymptotic relations (86) and (90) with $\Im L(0+{\rm i}kV,k) \leqslant 0$ (see Section 2.3). For mode I it is

$$L_+(0+{\rm i}kV,k) \sim \frac{L_0\mathscr{R}_{\rm I}}{\sqrt{0-{\rm i}k}}, \quad L_-(0+{\rm i}kV,k) \sim \frac{L_0}{\mathscr{R}_{\rm I}\sqrt{0+{\rm i}k}},$$

$$L_0 = \sqrt{\frac{32V^2\beta_1}{\sqrt{3}R^0}} \quad (L_h = L_0\mathscr{R}_{\rm I}) \tag{94}$$

and for mode II it is

$$L_+(0+{\rm i}kV,k) \sim \frac{L_0\mathscr{R}_{\rm II}}{\sqrt{0-{\rm i}k}}, \quad L_-(0+{\rm i}kV,k) \sim \frac{L_0}{\mathscr{R}_{\rm II}\sqrt{0+{\rm i}k}},$$

$$L_0 = \sqrt{\frac{32V^2\beta_2}{3\sqrt{3}R^0}} \quad (L_h = L_{\rm II}^0\mathscr{R}_{\rm II}), \tag{95}$$

where

$$\mathscr{R}_{\rm I,II} = \exp\left(\frac{1}{\pi}\int_0^\infty \frac{\operatorname{Arg} L_{\rm I,II}(0+{\rm i}\xi V,\xi)}{\xi}{\rm d}\xi\right). \tag{96}$$

Note that for $V > 0$ the upper limit of the integral is, in fact, a function of the speed since the integrand is a function of finite support (which increases as V decreases).

4.3.2. Super-Rayleigh speed, $c_{\rm R} < V < c_2$

Let us represent the function $L(0+{\rm i}\xi V,\xi)$ in the region $-1 < \xi < 1$ as

$$L(0+{\rm i}\xi V,\xi) = L^*(0+{\rm i}\xi V,\xi)l(\xi), \quad l(\xi) = \frac{0-{\rm i}\xi}{0+{\rm i}\xi}. \tag{97}$$

It follows (see Eqs. (87) and (91)) that

$$\operatorname{Arg} L^* = 0(\xi = 0), \quad |l(\xi)| = 1, \quad \operatorname{Arg} l(\xi) = -\pi\operatorname{sgn}\xi. \tag{98}$$

Using the Cauchy-type integral (63) for both functions, L^* ($L^*=L$ for $|\xi|>1$) and $l(\xi)$ one obtains the following asymptotes for $k\to 0$:

$$l=l_+l_-,\quad l_+=\exp\left(\frac{1}{2\pi\mathrm{i}}\int_{-1}^{1}\frac{\ln l(\xi)}{\xi-k}\mathrm{d}\xi\right)\sim(0-\mathrm{i}k)\quad(\Im k>0),$$

$$l_-=\exp\left(-\frac{1}{2\pi\mathrm{i}}\int_{-1}^{1}\frac{\ln l(\xi)}{\xi-k}\mathrm{d}\xi\right)\sim(0+\mathrm{i}k)^{-1}\quad(\Im k<0) \tag{99}$$

and

$$L_+\sim L_0\mathscr{R}_1(0-\mathrm{i}k)^{1/2},\quad L_-\sim\frac{L_0}{\mathscr{R}_1}(0+\mathrm{i}k)^{-3/2},$$

$$L_0=\sqrt{-\frac{32V^2\beta_1}{\sqrt{3}R^0}}\quad\text{(mode I)},\qquad L_0=\sqrt{-\frac{32V^2\beta_2}{3\sqrt{3}R^0}}\quad\text{(mode II)},$$

$$\mathscr{R}_1=\exp\left[\frac{1}{\pi}\left(\int_0^1\frac{\operatorname{Arg}L(\xi)+\pi}{\xi}\mathrm{d}\xi+\int_1^\infty\frac{\operatorname{Arg}L(\xi)}{\xi}\mathrm{d}\xi\right)\right], \tag{100}$$

where $\mathscr{R}_1$ is a speed-dependent function, $L_h=L_0\mathscr{R}_1$.

4.3.3. Intersonic speed

We use the regularization of the function $L(0+\mathrm{i}\xi V,\xi)$ in the region $-1<\xi<1$ similar to that for the super-Rayleigh case:

$$L(0+\mathrm{i}\xi V,\xi)=L^*(0+\mathrm{i}\xi V,\xi)l(\xi),$$

$$l(\xi)=l_{\mathrm{I}}(\xi)=\left(\frac{0-\mathrm{i}\xi}{0+\mathrm{i}\xi}\right)^{1/2+\omega}\quad\text{(mode I)},$$

$$l(\xi)=l_{\mathrm{II}}(\xi)=\left(\frac{0-\mathrm{i}\xi}{0+\mathrm{i}\xi}\right)^{\omega}\quad\text{(mode II)}. \tag{101}$$

It follows (see Eqs. (88) and (92)) that

$$\operatorname{Arg}L^*=0\ (\xi=0),\quad |l_{\mathrm{I,II}}(\xi)|=1,$$

$$\operatorname{Arg}l_{\mathrm{I}}(\xi)=-\pi(1/2+\omega)\operatorname{sign}\xi\quad\text{(mode I)},$$

$$\operatorname{Arg}l_{\mathrm{II}}(\xi)=-\pi\omega\operatorname{sign}\xi\quad\text{(mode II)}. \tag{102}$$

Using the Cauchy-type integral (63) for both functions, L^* ($L^*=L(|\xi|>1)$ and $l_{\mathrm{I,II}}(\xi)$ one obtains the asymptotes for mode I:

$$L_+\sim L_0\mathscr{R}_2(0-\mathrm{i}k)^{\omega},\quad L_-\sim\frac{L_0}{\mathscr{R}_2}(0+\mathrm{i}k)^{-\omega-1},$$

$$\mathscr{R}_{2\mathrm{I}}=\exp\left[\frac{1}{\pi}\left(\int_0^1\frac{\operatorname{Arg}L(\xi)+\pi(\omega+1/2)}{\xi}\mathrm{d}\xi+\int_1^\infty\frac{\operatorname{Arg}L(\xi)}{\xi}\mathrm{d}\xi\right)\right] \tag{103}$$

and for mode II:

$$L_+ \sim L_0\mathscr{R}_2(0-\mathrm{i}k)^{\omega-1/2}, \quad L_- \sim \frac{L_0}{\mathscr{R}_2}(0+\mathrm{i}k)^{-\omega-1/2},$$

$$\mathscr{R}_{2\mathrm{II}} = \exp\left[\frac{1}{\pi}\left(\int_0^1 \frac{\operatorname{Arg} L(\xi)+\pi\omega}{\xi}\mathrm{d}\xi + \int_1^\infty \frac{\operatorname{Arg} L(\xi)}{\xi}\mathrm{d}\xi\right)\right], \tag{104}$$

where

$$L_0 = \sqrt{\frac{32V^2\beta_1}{\sqrt{3}T}} \quad \text{(mode I)}, \qquad L_0 = \sqrt{\frac{32V^2\beta_2^*}{3\sqrt{3}T}} \quad \text{(mode II)}. \tag{105}$$

4.3.4. Supersonic speed

Using the same procedure one obtains (see Eqs. (89) and (93))

$$L_+ \sim L_0\mathscr{R}_3, \quad L_- \sim \frac{L_0}{\mathscr{R}_3}(0+\mathrm{i}k)^{-1},$$

$$L_0 = \sqrt{\frac{32V^2\beta_1^*}{\sqrt{3}R^{00}}} \quad \text{(mode I)}, \qquad L_0 = \sqrt{\frac{32V^2\beta_2^*}{3\sqrt{3}R^{00}}} \quad \text{(mode II)},$$

$$R^{00} = 4\beta_1^*\beta_2^* + (1+\beta_2^2)^2 \tag{106}$$

and

$$\mathscr{R}_3 = \exp\left[\frac{1}{\pi}\left(\int_0^1 \frac{\operatorname{Arg} L(\xi)+\pi/2}{\xi}\mathrm{d}\xi + \int_1^\infty \frac{\operatorname{Arg} L(\xi)}{\xi}\mathrm{d}\xi\right)\right]. \tag{107}$$

4.4. The energy release

It can be seen that for $h_+ = r_- = 0$ the second condition in Eq. (66) is not satisfied, while the first condition is satisfied in the sub-Rayleigh region, $0 < V < c_\mathrm{R}$, for both modes and in the intersonic region, $c_2 < V < c_1$, for mode II. In other cases the macrolevel-associated solution does not exist. Consider both favourable cases.

4.4.1. Sub-Rayleigh crack speed

In the considered sub-critical case, the global (macrolevel) energy release rate is defined by the macrolevel asymptote of the solution. The nondimensional energy release rate is defined as a limit:

$$G = \lim_{p\to\infty} p^2 Q_-(-\mathrm{i}p)Q_+(\mathrm{i}p). \tag{108}$$

This formula is valid for both the local (microlevel) and the global (macrolevel) energy release rate. The difference lies in the expressions for $Q_\pm$. In the considered case of a zero wavenumber, exponent μ in Eq. (66) is negative and only the first term in each of expressions (70) remains. Formula (108) defines the local energy release rate as

$$G_0 = Q^2(0) = L_h^2 q_h^2 = L_0^2 q_h^2 \mathscr{R}_1^2. \tag{109}$$

The global energy release rate, G, is represented in terms of the long-wave asymptotes of $Q_{\pm}(k)$ ($k \to 0$). Referring to Eqs. (70) and (94)–(96) we have the macrolevel solution

$$Q_+ \sim \frac{L_h q_h}{L_+(k)(0-\mathrm{i}k)} = \frac{q_h}{\sqrt{0-\mathrm{i}k}}, \quad Q_- \sim \frac{L_h q_h L_-(k)}{0-\mathrm{i}k} = L_0^2 q_h (0+\mathrm{i}k)^{-3/2},$$

$$Q(\eta) \sim \frac{q_h}{\sqrt{\pi\eta}} \quad (\eta > 0), \qquad Q(\eta) \sim L_0^2 q_h \sqrt{-2\eta/\pi} \quad (\eta < 0) \tag{110}$$

and the global energy release rate is

$$G = L_0^2 q_h^2. \tag{111}$$

Thus the energy release ratio is

$$\frac{G_0}{G} = \mathscr{R}_1^2. \tag{112}$$

Note that $\mathscr{R}_1 \leqslant 1$ since $\operatorname{Arg} L(0+\mathrm{i}\xi V, \xi) \leqslant 0$ as shown in Section 2.3. From the physical point of view, this inequality is a manifestation of the dissipative waves which carry a part of the global energy release away from the crack. This ratio for modes I and II together with that for mode III is shown in Fig. 6 of Part I of the paper (Slepyan, 2001a).

4.4.2. Mode II intersonic crack speed

The asymptotes ($k \to 0$) of solution (110) for the considered intersonic case are (see Eq. (104))

$$Q_+ \sim q_h (0-\mathrm{i}k)^{-\omega-1/2}, \quad Q_- \sim q_h L_0^2 (0+\mathrm{i}k)^{-\omega-3/2} \tag{113}$$

with the originals

$$Q(\eta) \sim q_h \frac{\eta^{-1/2+\omega}}{\Gamma(1/2+\omega)} \quad (\eta > 0), \qquad Q(\eta) \sim q_h L_0^2 \frac{(-\eta)^{1/2+\omega}}{\Gamma(3/2+\omega)} \quad (\eta < 0). \tag{114}$$

The global energy release rate can be calculated as a limit ($s' \to 0$) of the corresponding work of the force (see Eq. (67))

$$q = -q_h (2a_+ s')^{\nu} \exp(a_+ s' \eta) H(-\eta), \tag{115}$$

where for the considered case $\nu = 1/2 - \omega$. The work is

$$G = \lim_{s' \to +0} \int_{-\infty}^{0} q \frac{\mathrm{d}Q(\eta)}{\mathrm{d}\eta} \mathrm{d}\eta = L_0^2 q_h^2 \lim_{a_+ s' \to +0} (a_+ s')^{-2\omega}. \tag{116}$$

There exists a special case, $V = \sqrt{2} c_2$, where $\omega = 0$ and the solution is of the square-root type. In this case,

$$Q(\eta) \sim q_h / \sqrt{\pi\eta} \quad (\eta > 0),$$

$$Q(\eta) \sim q_h L_0^2 \sqrt{-2\eta/\pi} \quad (\eta < 0) \tag{117}$$

and

$$G_0 = Q^2(0) = L_h^2 q_h^2 = L_0^2 q_h^2 \mathscr{R}_2^2,$$

$$G_0/G = \mathscr{R}_2^2 \quad (V = \sqrt{2} c_2) \tag{118}$$

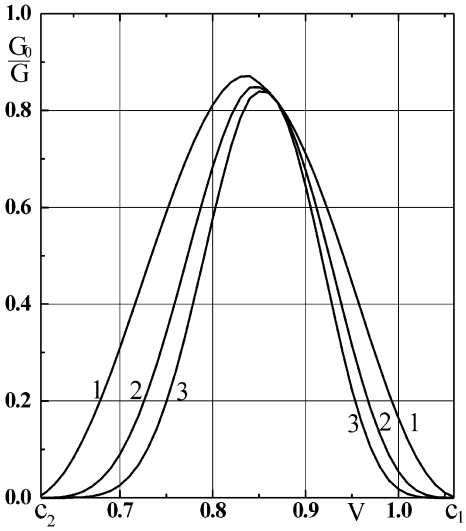

Fig. 9. The local-to-global energy-release ratio, G_0/G, for the intersonic crack speed: (1) $\gamma = 10^{-3}$; (2) $\gamma = 10^{-6}$; (3) $\gamma = 10^{-9}$.

with

$$\mathscr{R}_2 = \mathscr{R} = \exp\left(\frac{1}{\pi}\int_0^{\infty} \frac{\operatorname{Arg} L(\xi)}{\xi}\right). \tag{119}$$

The magnitude of $\mathscr{R}_2$ for $V = \sqrt{2}c_2$ can be found in Fig. 9 (it corresponds to the crossing point of the curves). Thus, in this special case, the energy release ratio, G_0/G, is finite, otherwise, $G = +\infty$.

The infinite work required for the intersonic crack propagation is, however, a characteristic of the macrolevel solution. This solution for the x-, y-plane can be found if one considers the problem on the macrolevel, that is in the framework of the homogeneous model. In terms of the scalar potential, ϕ, and the out-of-plane component of the vector potential, ψ, the solution is

$$\begin{aligned} &\phi = A\Im(\eta + i\alpha_1 y)^{\omega+3/2}, \\ &\psi = B(-\eta - \beta_2^* y)^{\omega+3/2} H(-\eta - \beta_2^* y), \\ &B = A\frac{1+\beta_2^2}{2\beta_2^*}\cos\pi\omega, \end{aligned} \tag{120}$$

where A is an arbitrary constant. The displacements are

$$u_x = \frac{\partial\phi}{\partial x} + \frac{\partial\psi}{\partial y}, \qquad u_y = \frac{\partial\phi}{\partial y} - \frac{\partial\psi}{\partial x}. \tag{121}$$

It can be easily seen that this solution satisfies the corresponding wave equations as well as the homogeneous conditions at the upper half-plane boundary, $y = +0$: $\sigma_{yy} = 0$ $(-\infty < \eta < \infty)$, $\sigma_{yx} = 0$ $(\eta < 0)$, $u_x = 0$ $(\eta > 0)$.

Note that the same result can be obtained as a proper continuation of the long-wave asymptote of the macrolevel-associated lattice solution (114) from $y=0$ to $y>0$.

The total energy flux in the shear wave represented by potential ψ is infinite and this results in the infinite global energy release rate. In the special case where $V=\sqrt{2}c_2$, the shear wave disappears (see Eq. (120) with $\beta_2^2=-1$) and the global energy release rate becomes finite.

The macrolevel-associated lattice solution differs from this on the microlevel: a finite part of the energy is taken away as the local energy release and, in addition, a finite part is carried away by a high-frequency dissipative wave considered below. The existence of the macrolevel-associated solution with a nonzero local energy release suggests the existence of an inhomogeneous finite-energy-release-ratio solution for any intersonic speed. This question is considered in the next section.

4.5. Mode II intersonic crack speed. Inhomogeneous problem

Consider Eq. (65) with the load

$$q=-q_0(2\gamma)^{1/2-\omega}\exp(\gamma\eta)H(-\eta),$$

$$q^{\mathrm{F}}=q_-^{\mathrm{F}}=-\frac{q_0(2\gamma)^{1/2-\omega}}{\gamma+\mathrm{i}k}, \tag{122}$$

where γ is a small positive number. We can rewrite the right-hand side of Eq. (65) in the following form:

$$C=\left(\frac{1}{L_-(k)}-L_+(k)\right)q^{\mathrm{F}}=C_++C_-,$$

$$C_+=[L_+(\mathrm{i}\gamma)-L_+(k)]q^{\mathrm{F}},\quad C_-=\left[\frac{1}{L_-(k)}-L_+(\mathrm{i}\gamma)\right]q^{\mathrm{F}}. \tag{123}$$

It follows that

$$Q_+=\frac{C_+}{L_+},\ Q_-=C_-L_-. \tag{124}$$

Since γ is assumed to be small, we may use the asymptotic expressions (104) for $L_+(\mathrm{i}\gamma)$ and write

$$L_+(\mathrm{i}\gamma)\sim L_0\mathscr{R}_2\gamma^{\omega-1/2}\quad(0<\gamma\ll 1). \tag{125}$$

The local energy release rate is as before

$$G_0=\lim_{k\to\mathrm{i}\infty}(-\mathrm{i}k)^2Q_+^2\sim L_0^2q_0^2\mathscr{R}_2^2. \tag{126}$$

The global energy release rate can be calculated using the Parseval equality. Taking into account Eqs. (104) and (122)–(125) we find

$$G\sim\frac{1}{2\pi}\int_{-\infty}^{\infty}[\mathrm{d}Q(\eta)/\mathrm{d}\eta H(-\eta)]^{\mathrm{F}}\,\overline{q^{\mathrm{F}}(k)}\,\mathrm{d}k$$

$$=q_0^2 2^{1-2\omega}\gamma^{2-2\omega}\frac{1}{2\pi}\int_{-\infty}^{\infty}\frac{\mathrm{d}k}{\gamma^2+k^2}+2^{2-2\omega}\gamma^{1/2-\omega}\frac{L_0^2q_0^2}{2\pi}\int_{-\infty}^{\infty}\frac{(0+\mathrm{i}k)^{1/2-\omega}}{\gamma^2+k^2}\,\mathrm{d}k$$

$$= 2^{-2\omega} q_0^2 \gamma^{1-2\omega} + 2^{-2\omega} \frac{1}{\pi} \Gamma\left(\frac{3}{4} - \frac{\omega}{2}\right) \Gamma\left(\frac{1}{4} + \frac{\omega}{2}\right) \cos\left[\frac{\pi}{2}\left(\frac{1}{2} - \omega\right)\right] \gamma^{-2\omega} L_0^2 q_0^2. \tag{127}$$

For small γ the first term is negligible; thus the energy release ratio is

$$\frac{G_0}{G} \sim \frac{\pi}{\Gamma(\frac{3}{4} - \omega/2)\Gamma(\frac{1}{4} + \omega/2)\cos[\pi/2(\frac{1}{2} - \omega)]} (2\gamma)^{2\omega} \mathscr{R}_2^2. \tag{128}$$

It can be seen in Fig. 9 that the ratio, G_0/G, remains finite, that is not too small, in a vicinity of the point $V = V_* = \sqrt{2}c_2$ even for very small γ ($\gamma = 10^{-3}, 10^{-6}$ and 10^{-9}), where the feeding wave and the external load can be referred to the macrolevel (remind that the length unit is the 'interatomic' distance). Thus the lattice model admits the macrolevel-associated solution for intersonic crack speed in the shear-longitudinal wave-speed region, while in a cohesive-zone-free homogeneous-material model it exists only for the single speed, V_*. This difference is caused by the fact that, in the homogeneous model, the local energy release is possible only in the case of the square-root-type singularity, while for the shear-longitudinal wave-speed region the singularity is weaker. In contrast, the local energy release in the lattice, as well as in the cohesive zone model, is not connected with the singularity of the macrolevel field at all.

4.6. Dissipative waves

The dissipative waves are defined as contributions of nonzero singular points of $1/L_+$ and L_- (see Eq. (70)). Each of such waves is located ahead (behind) the crack front if its group velocity is greater (lower) than the phase velocity. Indeed, as was already noted, the function L_+ (L_-) incorporates the wavenumbers with $V_g > V$ ($V_g < V$). Thus these waves carry energy away from the crack front and can be called the *dissipative* waves. Consider the sub-Rayleigh (modes I and II) and the intersonic (mode II) regions.

4.6.1. Sub-Rayleigh crack speed, mode I

It can be seen in Fig. 2 that the function $1/L_+$ has one nonzero singular point in a region where, approximately, $0.218 < V < 0.254$ and one or more such points for $V < 0.207$. These points are of the square-root type, $1/\sqrt{0 - \mathrm{i}(k - r_+)}$, since they represent zeros of r_Δ. Note that the Rayleigh nonzero wavenumber is a regular point for $1/L_+$ and the Rayleigh wave cannot propagate to the right (of course, this also follows from the absence of a free boundary ahead the crack). In accordance with the type of the singular point, it decreases asymptotically (far from the crack front) as $1/\sqrt{\eta}$ ($\eta > 0$).

The function L_- has three or more nonzero singular points for any sub-Rayleigh crack speed. The corresponding dissipative waves carry energy to the left. A *fast-decreasing wave* corresponds to a singular point of type $\sqrt{0 + \mathrm{i}(k - r_-)}$. It decreases asymptotically (at $y = 0$) as $(-\eta)^{-3/2}$ ($\eta < 0$). Note that the fast-decreasing asymptote is true only on the crack surfaces. For a ray inclined to the crack line, one can expect that the decrease is of a square-root type (see Part I, Slepyan, 2001a). In addition, for $\eta < 0$

there exists the Rayleigh dissipative wave which corresponds to a simple pole of $L_-(k)$ as a singular point of type $1/(0+\mathrm{i}(k-h_+))$. This is a constant-amplitude wave, and h_+ is its wavenumber.

4.6.2. Sub-Rayleigh crack speed, mode II

In this case, the function $1/L_+$ has one or more nonzero singular points in the region where $V<0.239$, while function L_- has such points for any sub-Rayleigh crack speed (see Fig. 3). All the above discussed properties of the dissipative waves in mode I are valid for mode II as well.

4.6.3. Intersonic crack speed, mode II

In this region, the function L_- has one nonzero singular point for any V, while L_+ has no such point (see Fig. 3). Thus there exists only one microlevel dissipative wave in this case; it carries energy to the left. In addition, as already noted, a macrolevel shear wave plays an important role in the energy fluxes distribution (excluding the special case, $V=\sqrt{2}c_2$).

5. Microlevel solutions

5.1. General characterization

A microlevel solution is characterized by a feeding wave of a nonzero wavenumber. It is defined by the general solution (70) as well as the above-discussed macrolevel-associated solution. Both the feeding and dissipative waves are represented in Eq. (70). The waves of the first type are associated with the explicitly shown singular points $k=r_-$ in the expression for Q_+ and points $k=h_+$ in the expression for Q_-. They are characterized by an anomalous location relatively the crack front. To show this, consider a regular case where both functions h_Δ and r_Δ have only simple zeros, that is, there are no coincident zero points where $V_g=V$. In this case, the point $k=r_-$ is not a singular or zero point of L_+ and the point $k=h_+$ is a regular point of L_-. So, these poles define constant-amplitude waves (denoted as Q_f^+ and Q_f^-)

$$Q_f^+(\eta)=\frac{q_r}{L_rL_+(r_-)}\exp(-\mathrm{i}r_-\eta)H(\eta),$$

$$Q_f^-(\eta)=q_hL_hL_-(h_+)\exp(-\mathrm{i}h_+\eta)H(-\eta). \tag{129}$$

In these expressions, in general, q_h and q_r are assumed to be complex. For $k\neq 0$ the group velocity, V_g, of the wave with $k=r_-$ (the wave is located at the right, ahead the crack front) is less than its phase velocity, V, whereas $V_g>V$ for the wave with $k=h_+$ located at the left. Because the group velocity is the energy flux velocity, these inequalities give evidence that each of these waves carries energy to the crack front and this is a reason to call it the *feeding* wave. Note that, under a given crack speed, not only one but several feeding waves can exist simultaneously. Some of them (with wavenumbers as r_-) are placed ahead the crack front and others (with wavenumber as h_+)—behind the front.

Also note that relations (129) are valid for a complex feeding wave associated with a positive zero point, $k=h_+$ or r_-. In addition, there exists a similar solution for the wave associated with the point $k=-h_+$ or $-r_-$. In sum, these solutions represent a real wave.

Consider, for example, the case where q_h is the feeding wavenumber. The real elongation of the bond at $\eta=0$ can be expressed as (see Eqs. (70) and (64))

$$\Re Q(0)=\Re \lim_{k\to \mathrm{i}\infty}(-\mathrm{i}k)Q_+(k)=\Re \lim_{k\to -\mathrm{i}\infty}(\mathrm{i}k)Q_-(k)=\Re(L_h q_h). \tag{130}$$

At the same time, the feeding wave amplitude is

$$A=|Q_f^-(\eta)|=|q_h L_h L_-(h_+)|. \tag{131}$$

Let the wavenumber, $k=h_+$, the phase velocity, V, and the amplitude, A, of the feeding wave be given as well as the fracture criterion, $\Re Q(0)=Q_*$. These conditions allow one to determine the constant q_h in solution (70), namely, if $L_h=|L_h|\exp(\mathrm{i}\alpha)$ then (here α and β are real numbers)

$$q_h=\frac{A}{|L_h L_-(h_+)|}\mathrm{e}^{\mathrm{i}\beta},\quad \cos(\alpha+\beta)=\frac{Q_*|L_-(h_+)|}{A}. \tag{132}$$

It follows that the amplitude has a lower boundary

$$Q_*|L_-(h_+)|\leqslant A<\infty. \tag{133}$$

In fact, there exists an upper boundary of the amplitude as well. It is defined by the strength of the other bonds of the lattice which have to carry the wave.

In a particular case where two of the zeros unite (in such a resonant point $V_g=V$), solution (129) do not exist since $L_+(r_-)=0$ or $L_-(h_+)=\infty$. However, a dissipative wave associated with the united zero points can exist. In this case, such doubled zero point is split by two simple zeros in the solution: one of them belongs to Q_+ (through L_+), while another belongs to Q_- (through L_-).

5.2. Sub-Rayleigh crack speed

First of all we note that the acoustic and optical dispersion curves represented as curves 2 and 3 in Figs. 2 and 3 correspond to feeding waves of r_--type, while the Rayleigh branch as curve 1 corresponds to h_+-type. For mode I it can be seen in Fig. 2 that the feeding wavenumber r_- can be represented by the longitudinal wave for any V, except two resonant speeds: $V\approx 0.218$ and 0.254, and by the optical-I branch for any speed. For mode II such wavenumber exists for any speed in both the shear wave and the optical-II branches (see Fig. 3). Wavenumber h_+ exists only for a low speed, $V<0.122$, for both modes. Thus the feeding wave ahead the crack can exist for any sub-Rayleigh crack speed, while it can be placed behind the crack front if $V<0.122$. In the last case, it is the Rayleigh feeding wave.

The dissipative waves are similar to that for the above-considered macrolevel-associated solution. In addition, there exists a contribution of the zero point, $k=0$. Referring to Eqs. (70), (94) and (95) one can find that this contribution is

$$Q_+\sim \mathrm{const}\sqrt{0-\mathrm{i}k},\quad Q_-\sim\frac{\mathrm{const}}{\sqrt{0-\mathrm{i}k}},$$

$$Q(\eta) \sim \frac{\text{const}}{\eta^{3/2}} \quad (\eta \to +\infty), \qquad Q(\eta) \sim \frac{\text{const}}{\sqrt{\eta}} (\eta \to -\infty). \tag{134}$$

This asymptote coincides with a super singular macrolevel solution which defines a zero energy release (in total, the corresponding wave does not transfer energy from the crack). Thus solution (134) describes a part of the field propagating together with the crack, but not a dissipative wave.

5.3. Super-Rayleigh crack speed

There are two, longitudinal-wave and optical-I feeding wavenumbers, both of r_--type, for mode I (see Fig. 2) and two, shear-wave and optical-II feeding wavenumbers of the same type for mode II (see Fig. 3). Eq. (70) yields the following contribution of the feeding wavenumber, $k = r_-$:

$$Q(\eta) = \frac{q_r}{L_r L_+(r_-)} \exp(-r_- \eta) \quad (\eta > 0),$$

$$Q(\eta) = \frac{q_r}{\sqrt{-\pi\eta}} \exp(-r_- \eta) \quad (\eta > 0). \tag{135}$$

The first is the feeding wave, while the second is the dissipative one of the same wavenumber. The total elongation at the crack tip, $\eta = 0$, from Eq. (70) is as follows:

$$Q(0) = \frac{q_r}{L_r}. \tag{136}$$

Along with the above-mentioned, there exists a dissipative wave associated with another nonzero singular point. It propagates at $\eta < 0$. In addition, there is a contribution of the zero point, $k = 0$. It is (see Eqs. (100))

$$Q_+ \sim -\frac{\mathrm{i} q_r}{r_- L_0 L_r \mathscr{R}_1} \frac{1}{\sqrt{0 - \mathrm{i}k}},$$

$$Q_- \sim \frac{\mathrm{i} q_r L_0}{r_- L_r \mathscr{R}_1} \frac{1}{(0 + \mathrm{i}k)^{3/2}}. \tag{137}$$

This asymptote coincides with the macrolevel super-Rayleigh solution which corresponds to a negative energy release. Consider this case in more detail.

The real parts of these solutions, which correspond to a sum of those for $k = \pm r_-$, are

$$\Re Q(0) = \frac{2\Re(q_r L_r)}{|L_r|^2},$$

$$\Re Q(\eta) = \frac{4 L_0 \Im(q_r L_r)}{\sqrt{\pi} \mathscr{R}_1 r_- |L_r|^2} \sqrt{-\eta} \quad (\eta < 0),$$

$$\Re Q(\eta) = -\frac{\Im(q_r L_r)}{\mathscr{R}_1 r_- |L_r|^2 L_0 \sqrt{\pi\eta}} \quad (\eta > 0). \tag{138}$$

Note that the last two expressions are different in sign that corresponds to a negative energy release. This is why the super-Rayleigh regime is not acceptable as a macrolevel solution. In our case, however, a microlevel feeding wave plays a dominant role in

delivering energy to the crack, the macrolevel wave is a dissipative wave now, and from the energy point of view the super-Rayleigh regime is not forbidden.

The relative values of the elongation are

$$S^- = \frac{Q(\eta)}{\sqrt{-\eta}Q(0)} = \frac{2L_0\Im(q_rL_r)}{\sqrt{\pi}r_-\mathscr{R}_1\Re(q_rL_r)},$$

$$S^+ = -\frac{Q(\eta)\sqrt{\eta}}{Q(0)} = -\frac{\Im(q_rL_r)}{\sqrt{\pi}r_-\mathscr{R}_1L_0\Re(q_rL_r)}, \tag{139}$$

where the function, L_r, obtained using the Cauchy-type integral with a regularization similar to that used above, is

$$L_r = \lim_{\xi\to r_-}\left[\frac{L(0+\mathrm{i}\xi V,\xi)}{\sqrt{0+\mathrm{i}(\xi-r_-)}}\right]^{1/2}\exp\left[-\frac{1}{2\pi i}(\phi_1+\phi_2)\right],$$

$$\phi_1 = V.p.\int_{r_--1}^{r_-+1}\frac{\ln[L(0+\mathrm{i}\xi V,\xi)/\sqrt{0+\mathrm{i}(\xi-r_-)}]}{\xi-r_-}\,\mathrm{d}\xi,$$

$$\phi_2 = -\frac{1}{2\pi i}\left(\int_{-\infty}^{r_--1}+\int_{r_-+1}^{\infty}\right)\frac{\ln L(0+\mathrm{i}\xi V,\xi)}{\xi-r_-}\,\mathrm{d}\xi. \tag{140}$$

Let us represent L_r and q_r as

$$L_r = |L_r|\mathrm{e}^{\mathrm{i}\alpha}, \quad q_r = |q_r|\mathrm{e}^{\mathrm{i}\beta}, \tag{141}$$

where α is a speed-dependent constant defined by Eq. (140) and β is a free constant (it depends on the position of the crack front relatively the wave, that is depends on the ratio $|q_r|/Q_*$, $Q_* = Q(0)$). Then

$$S^- = \frac{2L_0}{\sqrt{\pi}r_-\mathscr{R}_1}\tan(\alpha+\beta),$$

$$S^+ = -\frac{1}{\sqrt{\pi}r_-L_0\mathscr{R}_1}\tan(\alpha+\beta). \tag{142}$$

It is clear that one of these ratios, for example the first of them, can be positive. This demonstrates that the super-Rayleigh solution can exist without crack face interpenetration.

5.4. Intersonic crack speed

Contrary to the macrolevel-associated solution, intersonic nonzero feeding wavenumbers exist not only for mode II but for mode I as well. As can be seen in Fig. 2, in the case of mode I, both the longitudinal-wave and the optical-I branches can represent a feeding wavenumber of r_--type for any speed in this range. These feeding waves are placed ahead the crack delivering energy from the right since $V_g < V$ for both waves. In the case of mode II, only the optical-II branch remains (see Fig. 3) with a feeding wavenumber of the same type.

The microlevel dissipative waves are similar to those for the above-considered macrolevel-associated solution. The contribution of the zero point is a fast-decreasing wave.

5.5. Supersonic crack speed

Microlevel feeding waves can provide supersonic crack propagation. Indeed, the optical-I branch in the case of mode I and as well as the optical-II branch in the case of mode II can represent the required wavenumber of r_--type. It follows from Eq. (70) that the supersonic feeding wave is

$$Q_+ = \frac{q_r}{L_r L_+(r_-)[0 - \mathrm{i}(k - r_-)]},$$

$$Q_f^+(\eta) = \frac{q_r}{L_r L_+(r_-)} \exp(-\mathrm{i}r_-\eta) H(\eta), \tag{143}$$

where the wavenumber, r_-, satisfies the equation

$$\Omega_3 = \sqrt{6}\cos(k/4) = kV \quad \text{(mode I) or}$$

$$\Omega_4 = [2\cos(k/4)^2 + 4\sin(k/2)^2]^{1/2} = kV \quad \text{(mode II)}. \tag{144}$$

A dissipative wave of the same wavenumber as the feeding wave exists in both cases. As follows from Eq. (70) it is

$$Q_- = \frac{q_r}{\sqrt{0 + \mathrm{i}(k - r_-)}},$$

$$Q(\eta) \sim \frac{q_r}{\sqrt{-\pi\eta}} \exp(-\mathrm{i}r_-\eta) \quad (\eta \to -\infty). \tag{145}$$

The zero wavenumber corresponds to a wave as a constant crack opening displacement at $\eta < 0$.

6. Conclusion

Crack propagation in the lattice is considered here as caused by a feeding wave and accompanied by dissipative waves. Note that the dissipative waves obey the causality principle which, in its narrow sense, states that the solution should contain only those waves which carry energy to infinity. This corresponds to the case where no energy sources at infinity are assumed. In a broad sense, this principle allows the waves which sources are prescribed by the problem formulation. The feeding waves, delivering energy to the crack tip from a remote source, obey just this broad-sense causality principle. Also note that the source 'at infinity' means, of course, that it is far removed from the crack tip in the structure scale.

We call the macrolevel-associated solution that which corresponds to a zero feeding wavenumber, while the microlevel solution, which has no analogue on the macrolevel, corresponds to a nonzero feeding wavenumber. The macrolevel-associated homogeneous solutions exist in two cases: in the sub-Rayleigh region, $0 < V < c_R$, for both modes and in the intersonic region, $c_2 < V < c_1$, for mode II. In other cases, such solutions do not exist. In contrast, the microlevel solutions exist for both modes in all cases as sub-Rayleigh, super-Rayleigh, $c_R < V < c_2$, intersonic and supersonic crack-speed regions.

The crack speed is considered as given that corresponds to cutting of the lattice rather than crack propagation. However, if remote external forces and the fracture criterion are given, the results allow one to determine the crack speed.

The possible wave configurations are defined by the dispersion relations (61) and (62), asymptotic expressions for the factors $L_{\pm}$ and the conditions concerning the existence of the macrolevel feeding waves (66). They are found here as steady-state solutions which satisfy the lattice dynamic equations, the crack faces conditions and the conditions of symmetry. Also, these solutions correspond to an arbitrary nonzero critical elongation of the bond (this condition is required to satisfy the criterion of the bond breaking). So, the results concerning the wave amplitude and displacements can be expressed through the critical elongation as a coefficient of proportionality, while the global energy release, as well as the energy of each wave, is proportional to the local energy release as the critical elongation energy.

Along with the above-mentioned conditions satisfied by the solutions, same additional restrictions can define whether a fracture regime can exist. Indeed, the fracture criterion must be first satisfied at the crack front and for the bond on the crack path; otherwise the steady-state solution cannot be applied to the crack propagation problem. Further, the solution must be stable. These questions were studied in Marder and Gross (1995). In particular, it was shown that a crack cannot propagate slowly since the first condition is not satisfied, and the steady-state solution is unstable for a fast crack in the sub-Rayleigh region. Note, however, that these conclusions concern only the elastic lattice under the critical elongation as a fracture criterion. Also note that a slow crack can exist in a viscoelastic lattice (see Slepyan et al., 1999; Slepyan, 2000). Next, a kinematic condition should be mentioned as the prohibition of the crack faces interpenetration. These additional restrictions should be taken into account in the examination of a specific problem.

The lattice model has demonstrated some scenarios and phenomena in fracture and phase transition which cannot be discovered in the framework of a homogeneous model. It would be interesting to consider these issues using a more realistic lattice model. Also, an application of the lattice approach to mechanical and electro-mechanical problems for thin films is seemed to be fruitful.

Acknowledgements

This research was supported by The Israel Science Foundation, grant No. 28/00-1, and ARO, Grant No: 41363-M.

References

Abraham, F.F., Gao, H., 2000. How fast can cracks propagate? Phys. Rev. Lett. 84 (14), 3113–3116.

Broberg, K.B., 1999. Cracks and Fracture. Academic Press, New York.

Burridge, R., Conn, G., Freund, L.B., 1979. The stability of rapid mode II shear crack with finite cohesive traction. J. Geophys. Res. 84, 2210–2222.

Freund, L.B., 1979. The mechanics of dynamic shear crack propagation. J. Geophys. Res. 84, 2199–2209.

Gao, H., Huan, Y., Gumbsch, P., Rosakis, A.J., 1999. J. Mech. Phys. Solids 47, 1941–1961.
Gerde, E., Marder, M., 2001. Friction and fracture. Nature 391, 37–42.
Kulakhmetova, Sh.A., Saraikin, V.A., Slepyan, L.I., 1984. Plane problem of a crack in a lattice. Mech. Solids 19, 101–108.
Marder, M., Gross, S., 1995. Origin of crack tip instabilities. J. Mech. Phys. Solids 43, 1–48.
Needleman, A., Rosakis, A.J., 1999. The effect of bond strength and loading rate on the conditions governing the attainment of intersonic crack growth along interfaces. J. Mech. Phys. Solids 47, 2411–2449.
Rosakis, A.J., Samudrala, O., Coker, D., 1999. Crack faster than the shear wave speed. Science 284, 1337–1340.
Rosakis, A.J., Samudrala, O., Singh, R.P., Shukla, A., 1998. Intersonic crack propagation in bimaterial systems. J. Mech. Phys. Solids 46, 1789–1813.
Slepyan, L.I., 1981. The Problem of the Propagation of a Cut at Transonic Velocity. Sov. Phys. Dokl. 26, 1192–1193.
Slepyan, L.I., 2000. Dynamic factor in impact, phase transition and fracture. J. Mech. Phys. Solids 48, 927–960.
Slepyan, L.I., 2001a. Feeding and dissipative waves in fracture and phase transition. I. Some 1D structures and a square-cell lattice. J. Mech. Phys. Solids 49, 469–511.
Slepyan, L.I., 2001b. Feeding and dissipative waves in fracture and phase transition. II. Phase-transition waves. J. Mech. Phys. Solids 49, 513–550.
Slepyan, L.I., Ayzenberg, M.V., Dempsey, J.P., 1999. A lattice model for viscoelastic fracture. Mech. Time-Dependent Mater. 3, 159–203.